RESEARCH PROGRAM ON CLOSED-CYCLE MAGNETOPLASMADYNAMIC ELECTRICAL POWER GENERATION WITH NON-EQUILIBRIUM IONIZATION

Semi-Annual Technical Summary Report

December 15, 1962 - June 15, 1963

MND - 3052

RESEARCH PROGRAM ON CLOSED-CYCLE MAGNETOPLASMADYNAMIC ELECTRICAL POWER GENERATION WITH NON-EQUILIBRIUM IONIZATION

Semi-Annual Technical Summary Report

December 15, 1962 - June 15, 1963

MND - 3052

Order Number:	326 and 327
Project Code Number:	9800
Date of Contract:	June 15, 1962
Contract Number:	Nonr-3866(00)
Contract Expiration Date:	December 31, 1963
Project Scientist:	Dr. M. E. Talaat, Phone 687-3800 Ext. 9607, Area Code 301
Contractor:	Martin Marietta Corporation Baltimore 3, Maryland

Approved by:

M. E. Talaat

M. E. Talaat, Manager
Energy Conversion R&D Laboratories
Nuclear Division

Martin Marietta Corporation
Baltimore 3, Maryland
July 1963

FOREWORD

This report presents the work accomplished under Contract Nonr-3866(00) for the period 15 December 1962 to 15 June 1963.

The research was carried out in the Energy Conversion R&D Laboratories of the Martin Marietta Corporation, Nuclear Division.

The program was carried out under the auspices of the Advanced Research Project Agency and the Power Branch of the Office of Naval Research and was sponsored by Dr. J. Huth of ARPA and Mr. J. A. Satkowski of ONR.

Table of Contents

I. INTRODUCTION

The objectives of this program are two: (1) to demonstrate experimentally the principle of non-equilibrium ionization under actual closed cycle magneto-plasmadynamic (MPD) generator operating conditions; and (2) to verify the basic phenomena underlying the behavior of moving ionized gases, in the non-equilibrium state, when interacting with a magnetic field. This will be done by correlating experimental results with the theory of non-equilibrium ionization.

To bring about these objectives, a three-part program is being carried out. In the first and major part an electrically heated, closed loop, experimental MPD electric power generator has been developed and fabricated for the purpose of evaluating the increase in output power density and electrical conductivity due to non-equilibrium ionization. It will also be used to evaluate the dependence of power generated in the MPD duct upon the thermodynamic state of the working fluid, the magnetic field strength, the electrode temperature, and the electrical load conditions. The working fluid will be a noble gas (helium seeded with cesium has been selected for the initial experiments), and it will operate at temperatures in the MPD generator duct within the approximate range of 1200 to 2000°K.

In support of the experimental part of this program and to guide in the selection of experimental conditions, as well as to correlate the experimental results with theory, two study programs are being carried out: one involving the process of non-equilibrium ionization; and the other involving the study and analysis of closed cycle MPD power generation under conditions compatible with the utilization of non-equilibrium ionization in the MPD duct.

All three parts of the program are thus directed toward demonstrating the success of non-equilibrium ionization under actual closed-cycle MPD power generator operating conditions. It is also aimed toward gaining an understanding of the basic important factors underlying the behavior of ionized seeded noble gases in the non-equilibrium state, and the application of these principles to MPD power generation at gas temperatures compatible with feasible nuclear reactor capabilities.

II. RESUME OF PROGRESS

During the first six months of the program* an experimental closed loop MPD electrical power generator was designed, and its major components were procured. In addition, a theory on MPD electrical power generation with non-equilibrium ionization (of seeded noble gases) was developed. Seeded noble gas-filled discharge tubes were made and tests were run to correlate experimental data with the developed theory.

During the second six months of the program the fabrication of the various components of the loop: namely, the helium plenum, the helium flow meter, the helium preheater, the helium main heater assembly complete with its six ceramic-to-metal sealed main current leads, the nozzle, the MPD duct assembly with its seven pairs of electrodes, pressure and temperature probes, the main cooler, the cesium separator, the after cooler, the surge tank, and all the interconnecting piping and valves, as well as the instrumentation and control panels, have been fabricated.

The MPD generator loop installation was completed, using at first a low temperature duct assembly capable of simulated operation at temperatures in the vicinity of 800°K. The purpose of this low temperature duct assembly is to complete the loop assembly so that initial leak checking and the outgassing of the entire loop (as well as the try out of instrumentation and controls) can proceed without any danger of contaminating the high temperature main heater-nozzle-generator duct-diffuser-exhaust assembly during the process. The low temperature assembly consists of a gas flow resistance section used to simulate the resistance to gas flow of the main heater, a low temperature nozzle section, a low temperature duct section lined with zirconia insulation (dimensions: 0.375" x 1.125" x 2.625") with four pairs of Mo electrodes, a diffuser section, and an exhaust pipe section.

* Semi-Annual Technical Summary Report (June 15 - December 15, 1962), MND-2939, On Research Program on Closed Cycle MPD Electrical Power Generation With Non-Equilibrium Ionization.

The loop assembly, using this low temperature duct, is now undergoing evacuation and leak checking. After location and repairing of leaks, certain components of the loop will be outgassed until a minimum evacuation pressure in the loop is attained. The loop will then be charged with the noble gas, the impurities monitored at gas temperatures up to 800°K in the duct, the loop purged of the gas and recharged until the level of impurities is at a minimum. The loop will then be operated in try-out runs at a gas temperature in the duct of 800°K to test the operation of the loop controls and determine the response of the instrumentation to variations in operating conditions. The operation of the cesium loop will also be checked out by circulating the cesium in bypass piping without mixing it with the helium gas. After the satisfactory completion of leak checking and the try-out phase, the low temperature duct assembly will be removed; and the high temperature generator duct assembly will be installed, evacuated, outgassed, purged, and charged with highest purity helium gas. The apparatus will then be ready for power generation during non-equilibrium ionization runs using stepwise raising of gas temperature and cesium seed injection.

The high temperature generator duct assembly consists of the tantalum-10% tungsten main heater assembly (with six ceramic-to-metal sealed main current leads), the high temperature nozzle, the MPD generator duct assembly (with alumina wall lining and seven pairs of iridium electrodes), pressure and temperature probes (with seven pairs of ceramic-to-metal sealed output power terminals), diffuser section, and exhaust section. These components are all protected by three series of stainless steel cover boxes which will be charged with a noble gas to prevent oxidation of the refractory metal components while operating at high temperatures.

During the past six month period, the heater design was improved to ensure against any high temperature reaction between the tantalum-10% tungsten heater elements and any zirconia insulation in their proximity. In addition, certain design improvements have been made and carried out 1) to ensure that the cover boxes and current and probe lead-throughs shall remain leak-tight, and 2) to prevent corrosion or a reaction with cesium should leaks between the gas flow and cover

box gas regions occur. These design improvements and added precautions were deemed necessary to allow longer trouble-free runs with cesium. The major assembly - consisting of the heater assembly, nozzle, duct assembly, diffuser, and exhaust sections, along with the protective cover box assemblies - is now undergoing final leak testing. It will be readied for installation after we have leak-checked the rest of the loop and have conducted satisfactory trial runs (referred to in previous paragraphs) with the low temperature duct assembly.

In the second part of the program (involving ionization studies) the theory of "MPD Electrical Power Generation With Non-Equilibrium Ionization" was applied in "A Comparison Between Test and Calculations of Non-Equilibrium Conductivities and the Corresponding Internal Electric Fields Required"**. Excellent agreement was obtained between tests and calculations based on the theory of non-equilibrium ionization developed during the first quarter period of the contract. In this theory the electron density is derived from an ion balance equation, and the electric field from an energy balance equation. Both theoretical calculations and experimental results obtained with a diode tube (containing helium seeded with about 0.5% cesium; helium density of 1.61×10^{24} atoms per cubic meter) show that electrical conductivities from 10 to about 150 mho/meter are obtained at current densities in the range of 1×10^{4} to 20×10^{4} amperes per sq meter and with electric fields in the range of 7×10^{2} to 12×10^{2} volts per meter, respectively. These values are of vital interest; and if they are realizable in MPD electrical power generation with non-equilibrium ionization, it would lead to output power densities on the order of tens to hundreds of megawatts per cubic meter of the generator duct. (For a more detailed report on this investigation see chapter IV of this report.)

---

* See Chapter III of the first semi-annual report, MND-2939.

** A ten minute paper presented before the 4th Symposium on the Engineering Aspects of Magnetohydrodynamics in Berkeley, California on April 11, 1963.

In the third part of the program, involving the study and analysis of closed cycle MPD power generation, the equations governing behavior of the ionized gas in the MPD duct have been solved for conditions compatible with the utilization of non-equilibrium ionization in the MPD duct. These solutions are presented in chapter V of this report for the case of a Faraday generator with segmented electrodes, operating with constant velocity or constant area duct and with constant electrical conductivity along the generator duct length. For compatibility with the principles of non-equilibrium ionization, the further condition is imposed: that, in order to maintain a certain conductivity under the non-equilibrium state, it is necessary to maintain constant the current density between each electrode pair and the corresponding internal electric field along the generator duct. To our knowledge, this is the first time the MPD generator equations have been solved for the constant area duct case under conditions compatible with the generation of non-equilibrium ionization conductivities. The results are presented in chapter V in normalized universal solutions to assist in their application to any examples of duct design, in performance prediction, or in correlation with theory.

III. EXPERIMENTAL CLOSED CYCLE MPD ELECTRICAL POWER GENERATOR

1. Introduction

The design of the experimental closed-cycle MPD electrical power generator was described in detail in the first semi-annual progress report (MND-2939). Copies of the design drawings of the overall equipment layout of the MPD experiment (J435A-6400014), the MPD instrumentation and control block diagram (E435A1367000), the helium plenum (E435-6400009), the main heater-nozzle-duct-diffuser-exhaust assembly (Fig. 12 of the first semi-annual report, MND-2939), the main cooler (J435A6400004), the cesium separator (E435-6400006), the after cooler (E4356400005) and the cesium accumulator (E435-6400015) were included in the same report (MND-2939). Pictures of the heater elements and plates (Figs. 4 and 11 of MND-2939), some of the components making up the heater and duct assemblies (Fig. 13 of MND-2939), the compressor piston and piston rod (Fig. 14 of MND-2939), the electromagnet (Fig. 16 of MND-2939) and the building housing the loop (Fig. 17 of MND-2939) were also included in the first semi-annual report.

2. Progress This Period

Since the beginning of this period, the helium plenum, the helium flow controls and helium flow meter, the helium preheater, the cesium injector, the main cooler, the cesium separator, the after cooler, the helium surge tank (ahead of the inlet to the compressor), the cesium storage tank, the cesium supply tank, the cesium pump, the cesium accumulator, the heated oil bath tank (housing the cesium tanks, cesium pump head and accumulator), the cesium flow controls, the cesium flow meter, and all the interconnecting piping and valves have been fabricated (or procured) and assembled in the loop. Compressor installation in the loop was completed by connecting the surge tank to the compressor inlet, by completing the pipe connection between the stages of the compressor, and then by connecting the compressor outlet to the helium plenum. The variable speed compressor drive was aligned with and coupled to the compressor shaft, and its

rotation and balance were tested. In addition, the instrumentation and control panel were fabricated, assembled, and initiated in the control room, located next to the loop.

The major subassembly, consisting of the main heater-nozzle - generator duct-diffuser-exhaust duct, together with the six ceramic-to-metal sealed main heater current leads, the fourteen ceramic-to-metal sealed generator duct output power leads, pressure and temperature probes and the three enclosing cover boxes for protection of the refractory metal parts, was completed on May 17, 1963. This represented a delay of about four weeks from the original schedule; and it was due primarily to difficulties encountered in fabrication of the six ceramic-to-metal sealed main heater current leads (seventeen days delay), and to incorporation of design improvements to ensure effective isolation of all the tantalum-10% tungsten parts (e.g. the heater elements, heater assembly box, nozzle support structure, generator duct assembly box, etc.) from any zirconia insulation blocks (eleven days delay). This design modification involved replacing the molybdenum isolation sheets (between the tantalum-10% tungsten material and the zirconia insulation) with tungsten isolation sheets. This increases the effectiveness of the isolation layer as a barrier to possible reaction between the tantalum-10% tungsten and the zirconia materials, particularly at higher temperatures (e.g. above 1800°K). The completed assembly was leak-checked during the week between May 17 and May 24 and leaks were located in some of the welds in the stainless steel cover boxes and in the tantalum-10% tungsten exhaust duct, as well as in two internal O-ring seals between the main gas stream region and the inert gas region inside the cover boxes. It was determined that repairing the leaks in the welds could be done readily and without significant delay while repairing the leaks in the two internal O-rings would involve a major "tear-up" operation, accompanied by considerable risk and an extensive delay in the schedule. On May 27, therefore, it was decided to proceed with repair of all leaks in the stainless steel and tantalum-10% tungsten welds. Moreover, since any leak between the main gas stream region and the inert gas regions under the cover

boxes would not be serious unless external room air leaked into the boxes and reacted with the refractory metals, it was concluded that the cover boxes should be made leak tight. To ensure this, it was decided to replace all brazed pressure and temperature probe or current lead-throughs in the cover box walls which might react with cesium (in case it leaked into the cover boxes inert gas regions from the main gas stream region), with leak-tight stainless steel welded pressure and temperature probe and current lead-throughs using insulation materials which would not react with or be corroded by cesium. These design improvements have been carried out, and at this writing, the major assembly (or the main heater-nozzle-generator duct-diffuser-exhaust duct together with the six ceramic-to-metal sealed main heater leads, the fourteen ceramic-to-metal sealed generator duct output power leads, pressure and temperature probes and the three enclosing cover boxes) is being rechecked for leaks.

Furthermore, it was decided to close the loop temporarily, using a low temperature duct assembly, in order to proceed with the evacuation, leak-checking, and outgassing of the remainder of the loop assembly. In addition, the use of the low temperature duct assembly would permit trying out the helium gas purging process and impurity monitoring procedure (using a chromatograph) - as well as the checkout of all the instrumentation and controls in trial runs at gas temperatures (in the duct) of about 800°K. This low temperature duct assembly is made of stainless steel and consists of a gas flow resistance section (to simulate the resistance to gas flow through the main heater), a low temperature nozzle section, a low temperature duct section lined with zirconia insulation (dimensions: 0.375" x 1.125" x 2.625") and having four pairs of molybdenum electrodes (0.375" x 0.375" each), a diffuser section, and an exhaust pipe section. The loop was closed with this low temperature duct assembly on June 24, and it is now being evacuated and leak-checked.

The following figures (Figs. 1 - 13) show the loop installation using the low temperature duct assembly, the compressor and compressor drive installation

the instrumentation and control panel, and the major assembly of the main heater-nozzle-generator duct-diffuser-exhaust duct and protective cover boxes in different stages of completion.

FIGURE CAPTIONS

Figure 1. MPD Loop Assembly - View Showing Low Temperature Duct between the Magnet Poles

Figure 2. MPD Loop Assembly - View Showing Exhaust Pipe, Cooler, Separator, After Cooler and the Oil Tank Housing Cesium Storage Tanks, Accumulator and Pump and Cooler

Figure 3. MPD Loop Assembly - View Showing the Compressor With Its Drive and the Surge Tank

Figure 4. MPD Loop Control Panel

Figure 5. MPD Generator Major Assembly Embodying the Main Heater Leads, the Main Heater, the Nozzle, the Generator Duct, the Diffuser, the Exhaust Duct and the Output Power Leads, and the Pressure and Temperature Probes

Figure 6. MPD Generator Major Assembly - View Without Cover Box on Main Heater Lead Seal Assemblies

Figure 7. MPD Generator Major Assembly - View Showing Output Power Leads, Pressure and Temperature Probes Coming Through the Cover Box

Figure 8. MPD Generator Major Assembly - View Showing the Output Power Leads and Refractory Ceramic-to-Metal Seals Inside the Cover Box

Figure 9. MPD Generator Major Assembly - View Showing Method of Assembling the Front Cover Box on the Main Heater Lead Seal Assemblies

Figure 10. Input Power Lead Seal Assembly

Figure 11. Heater Box and Element Assembly

Figure 12. Generator Electrodes and Insulation Components

Figure 13. Take-Off Seal and Flexible Lead Assembly

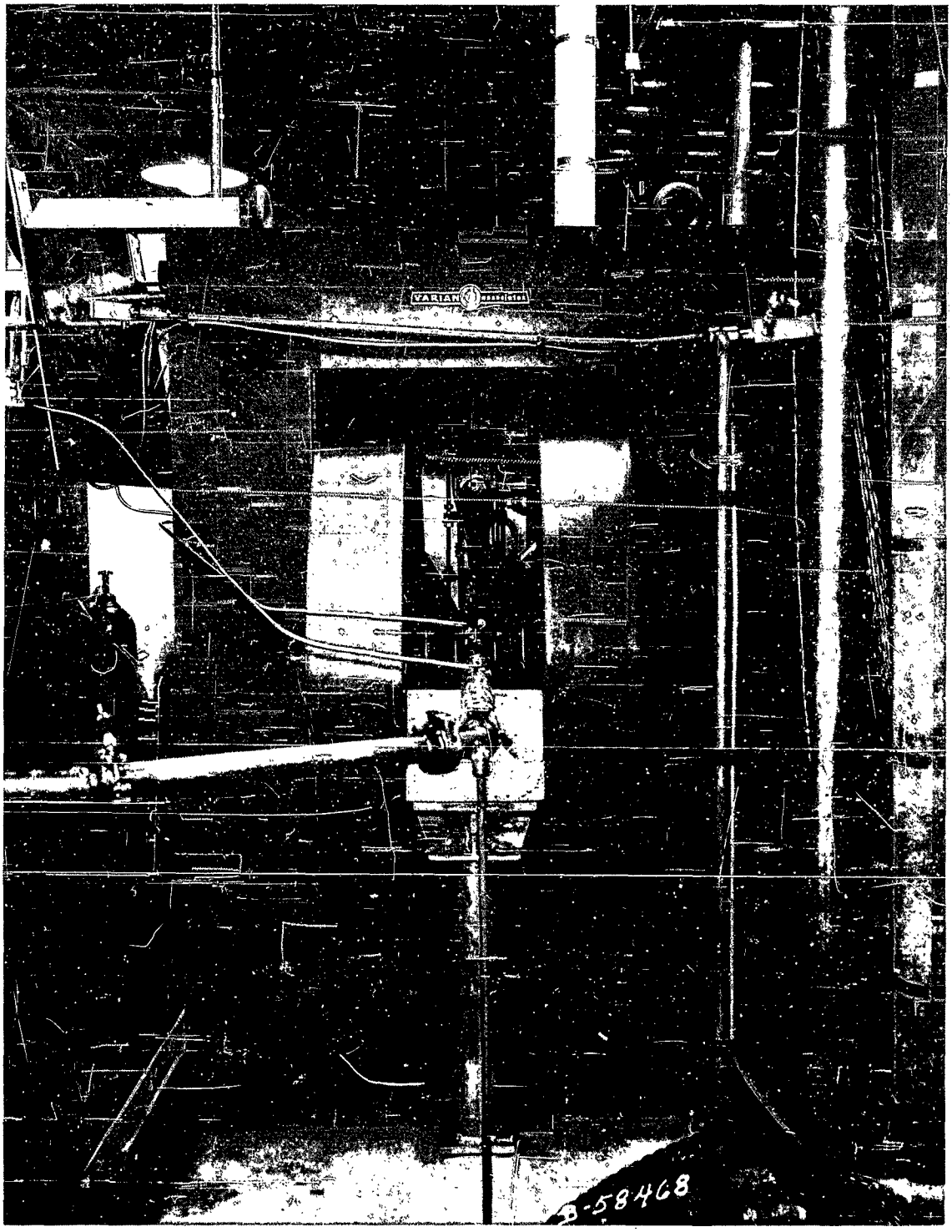
VARIAN
D-58468

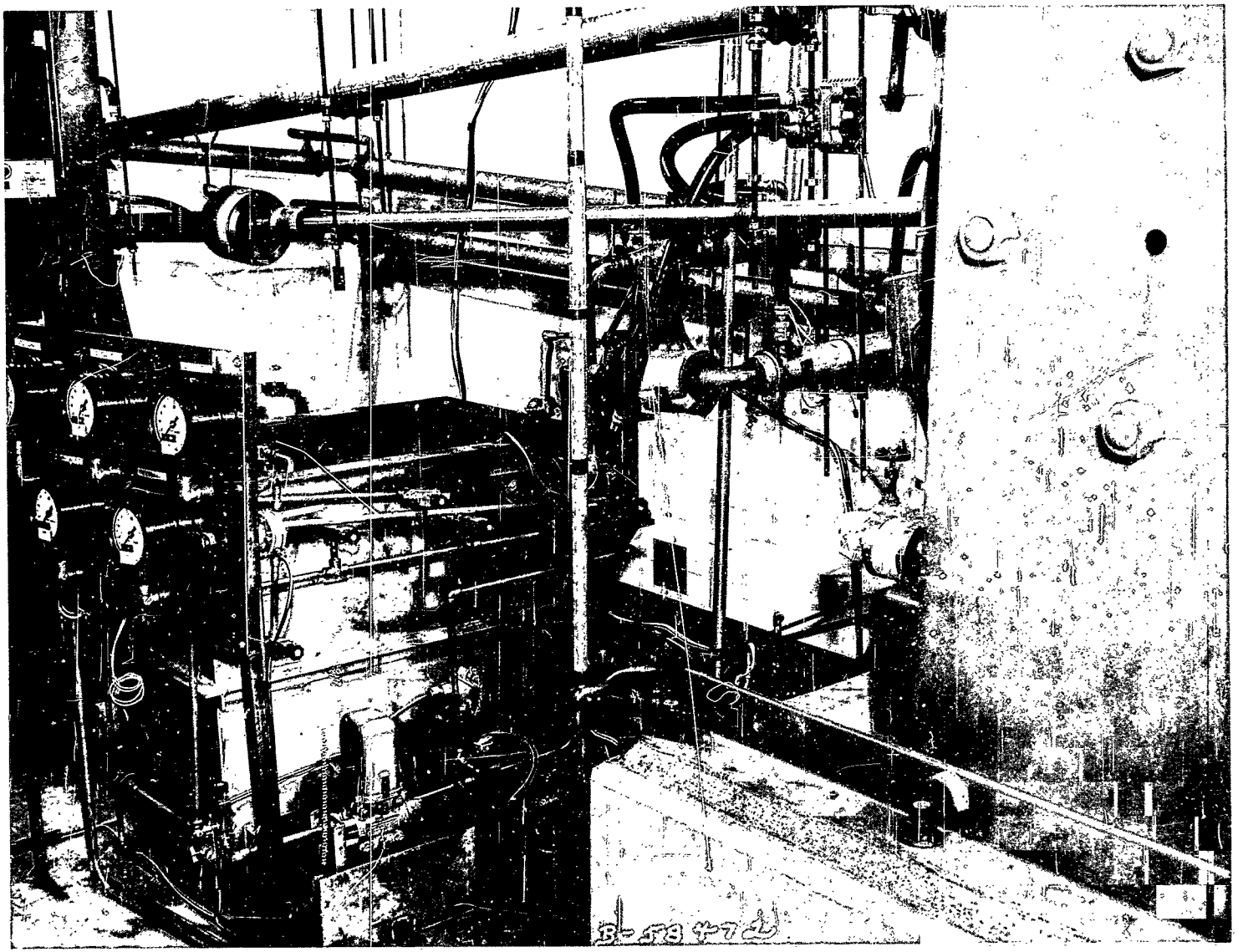
B-5F8 ヤフム

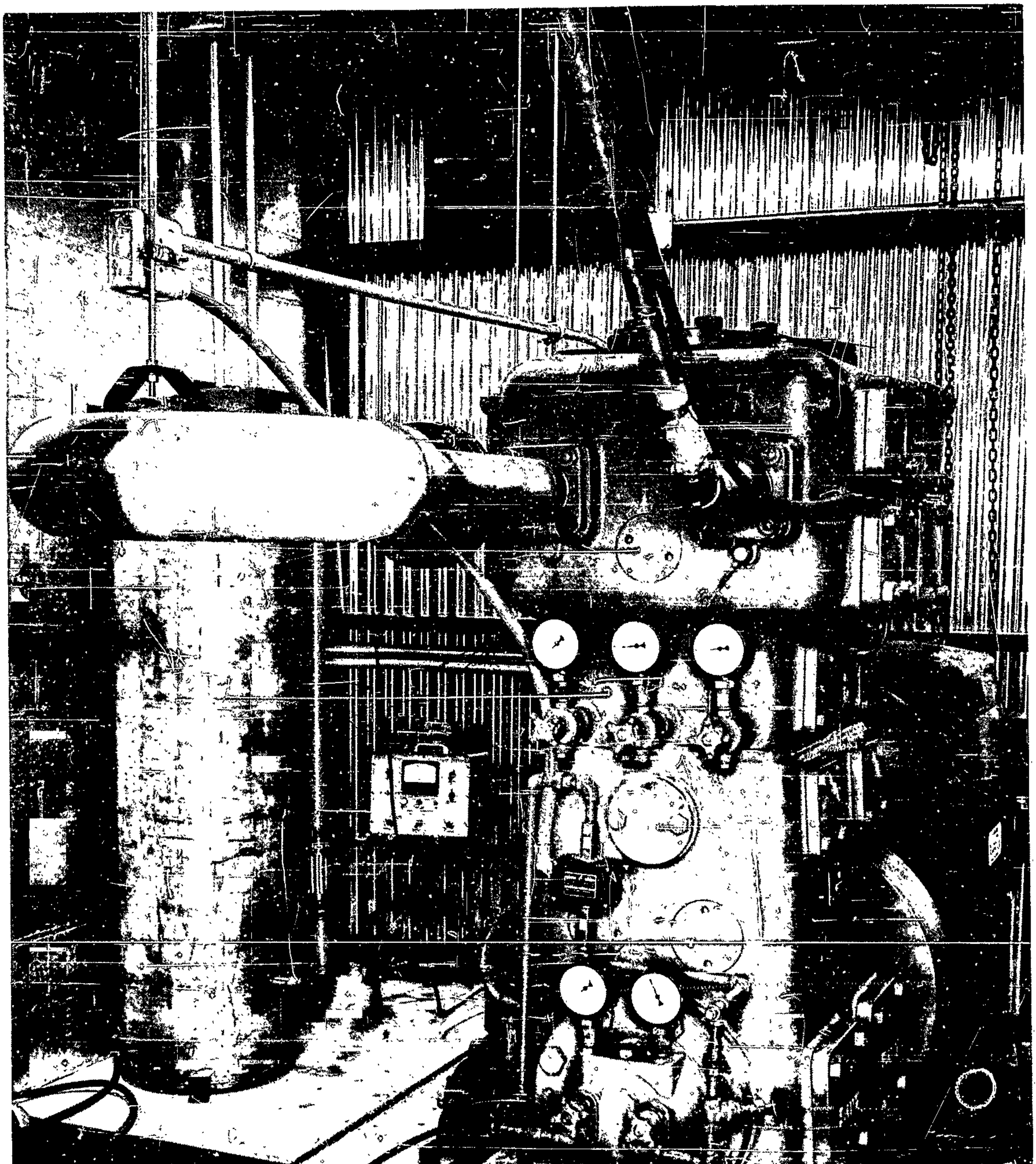

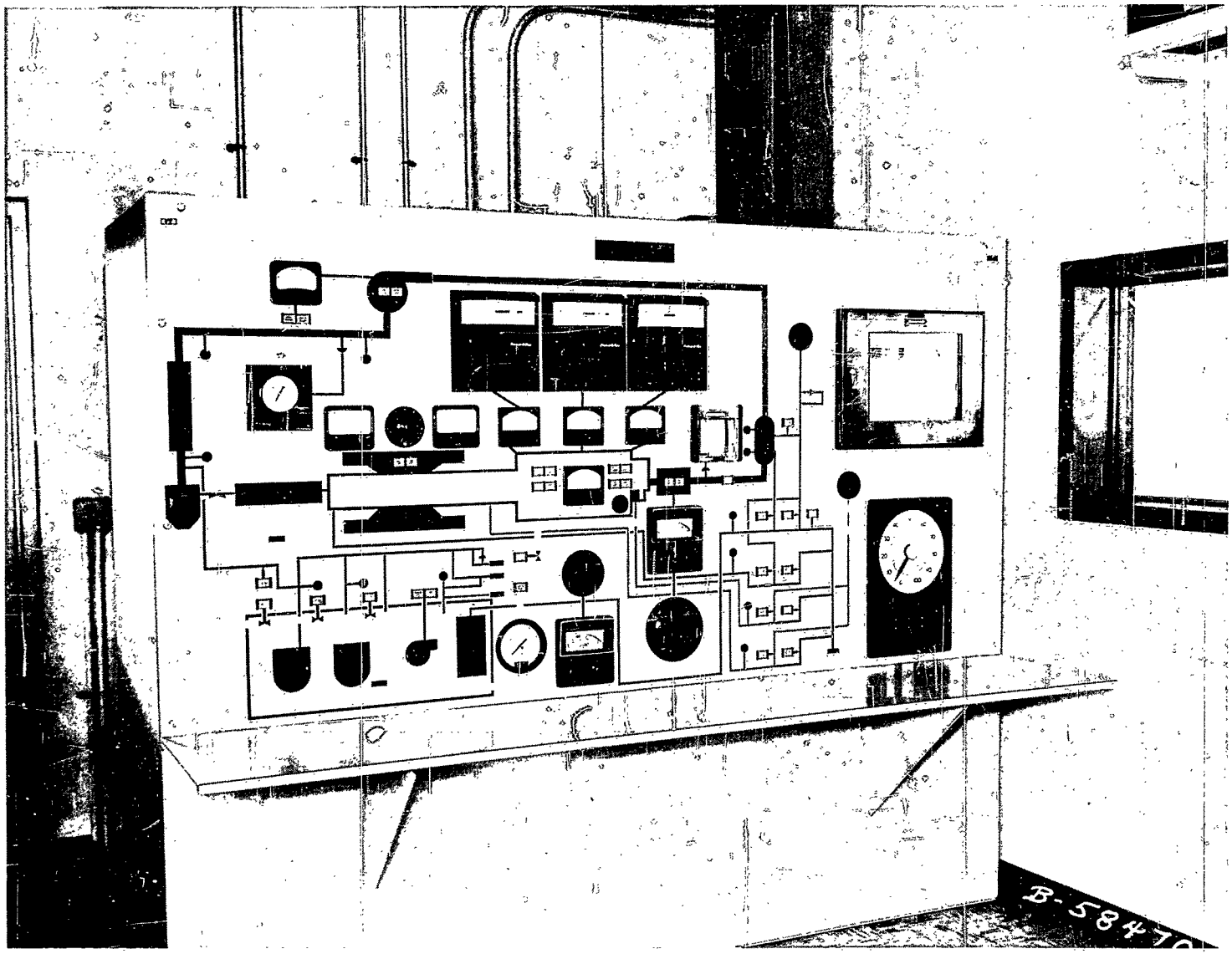
B-5847

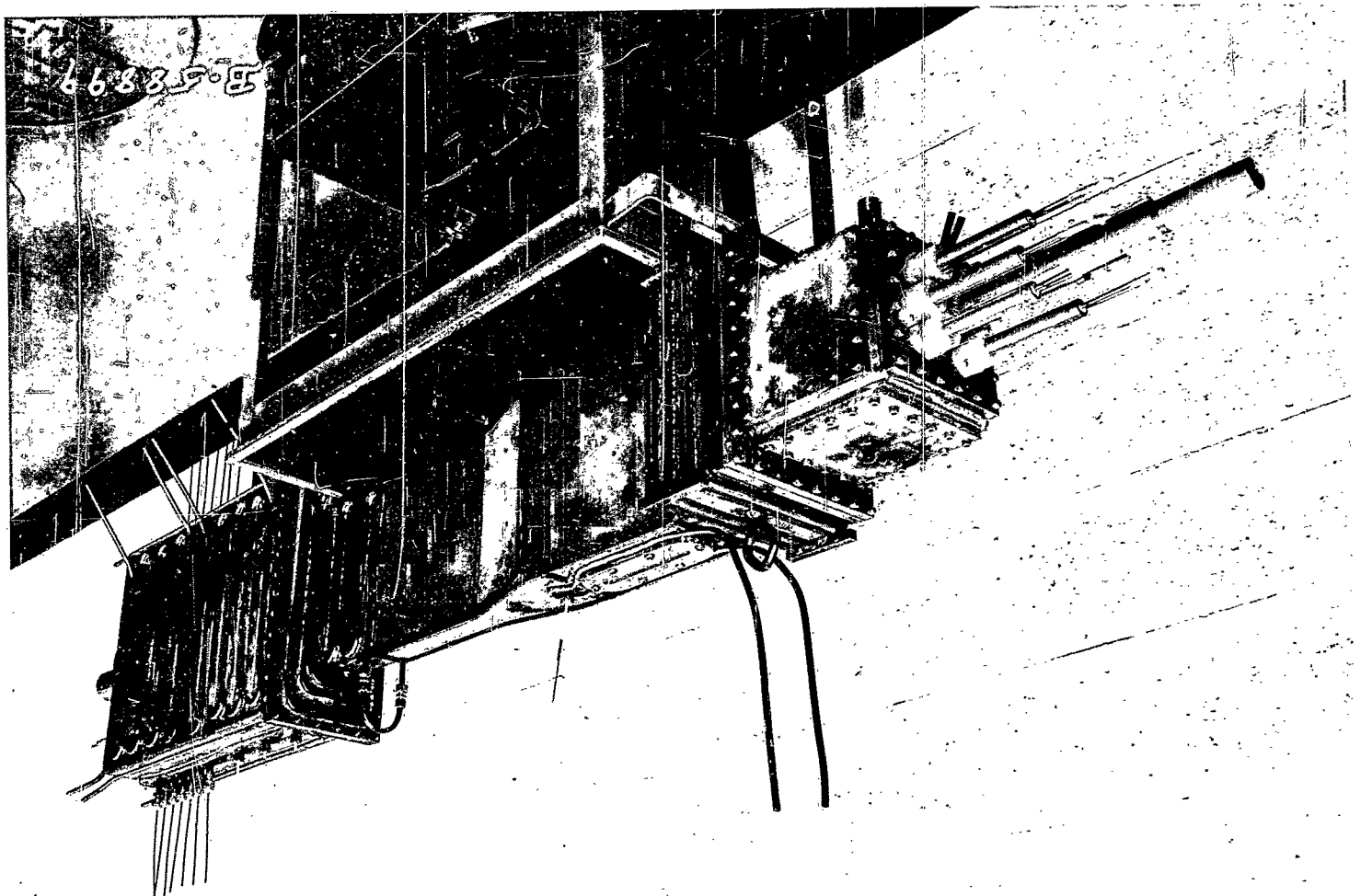

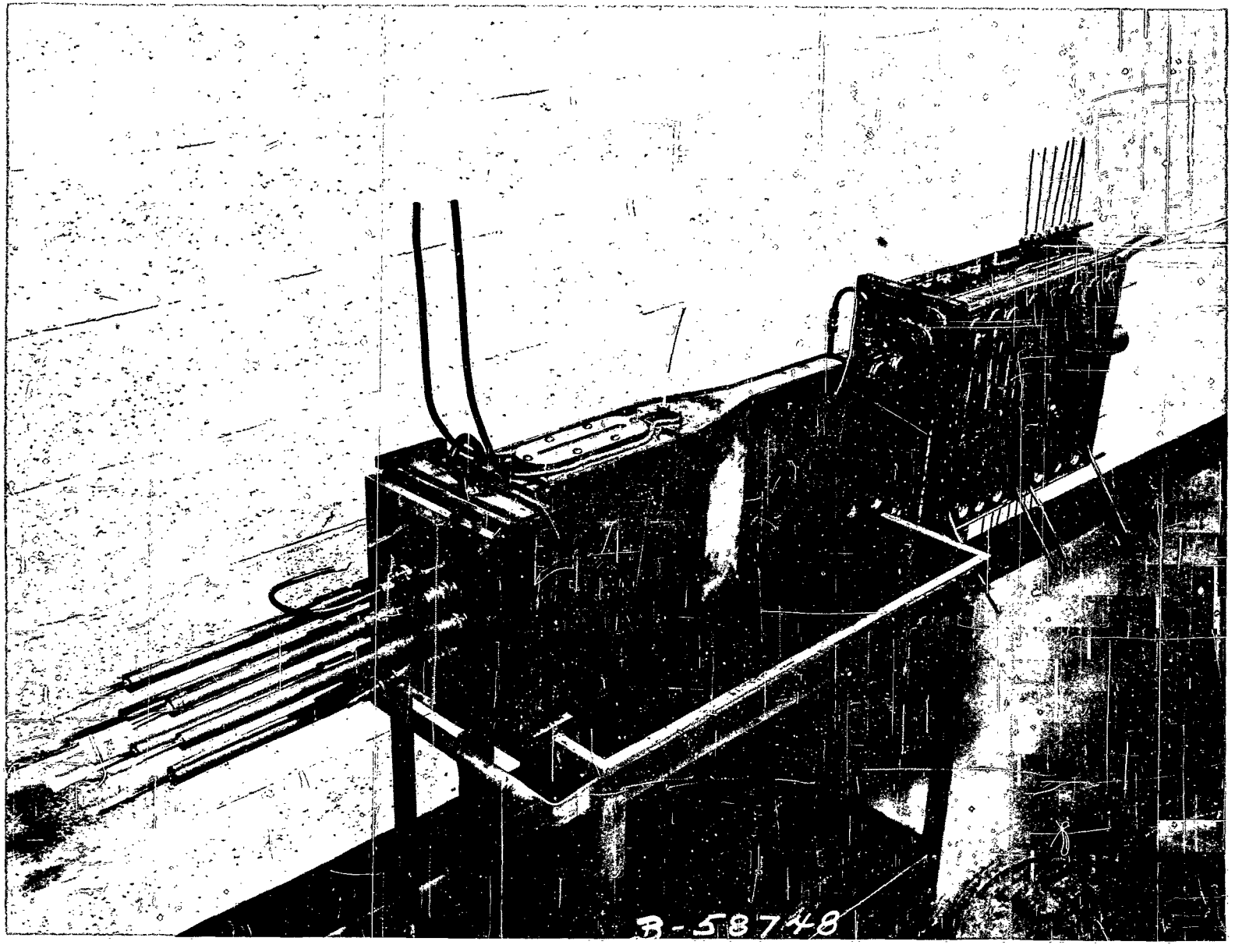
B-58748

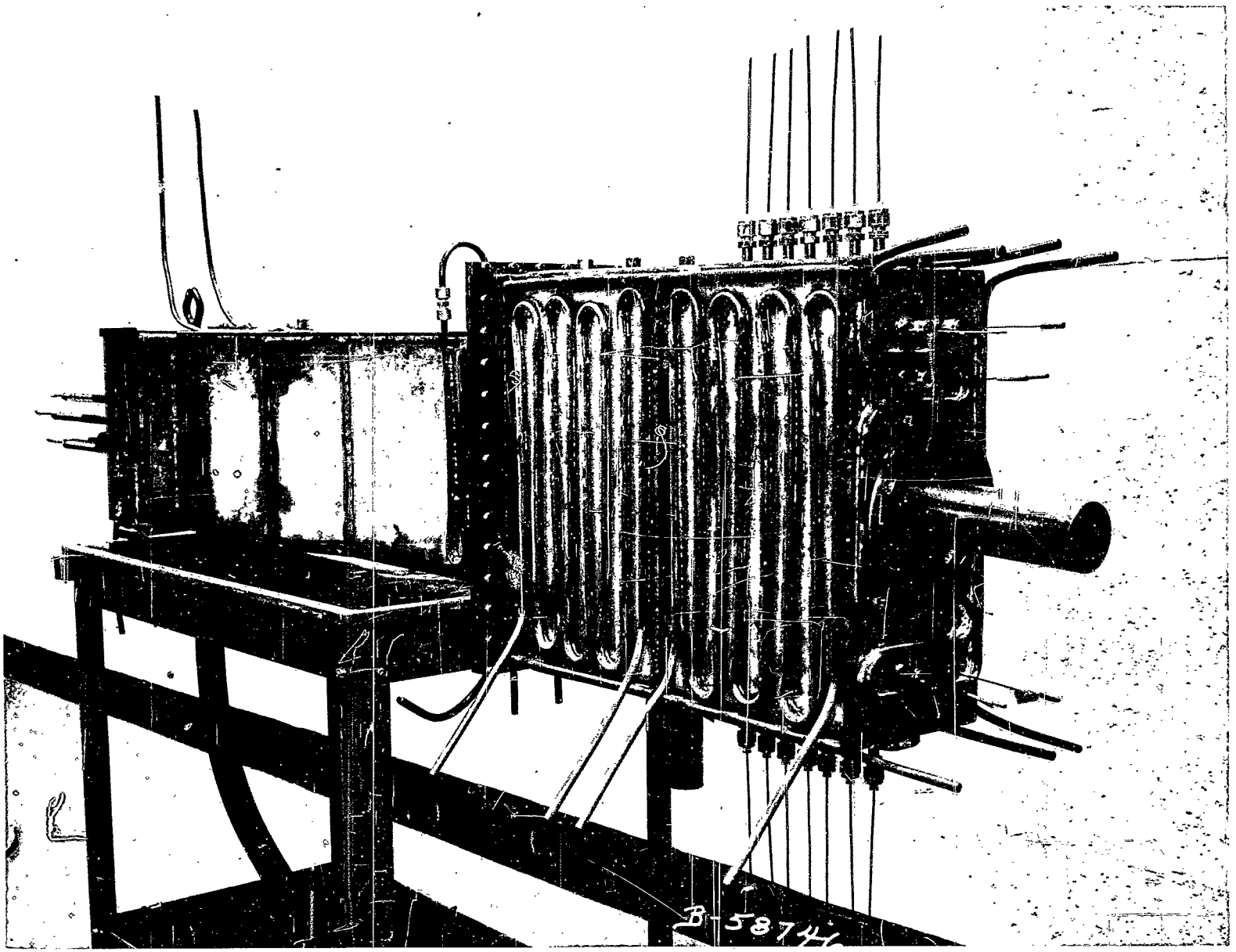
B-5874

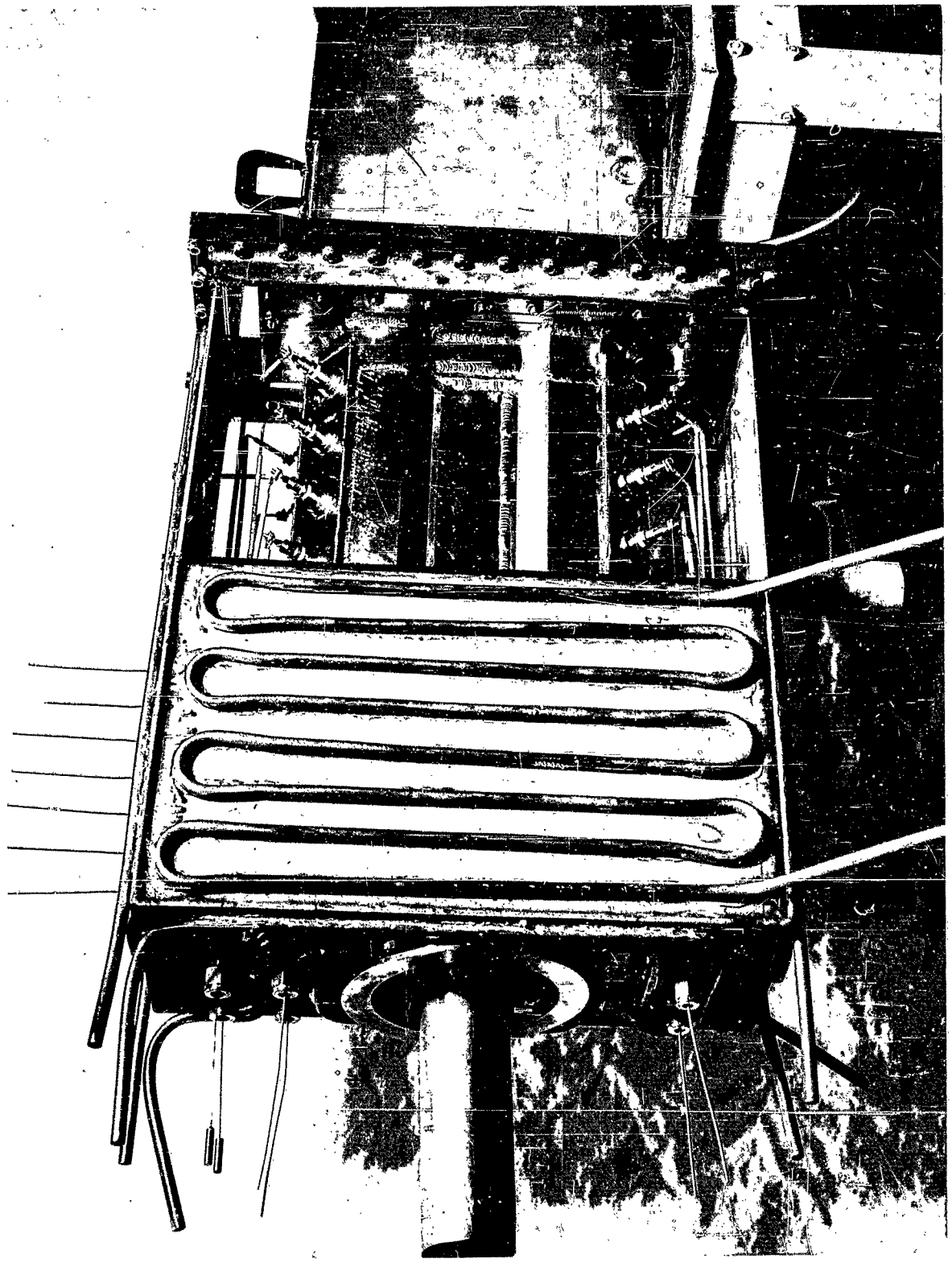

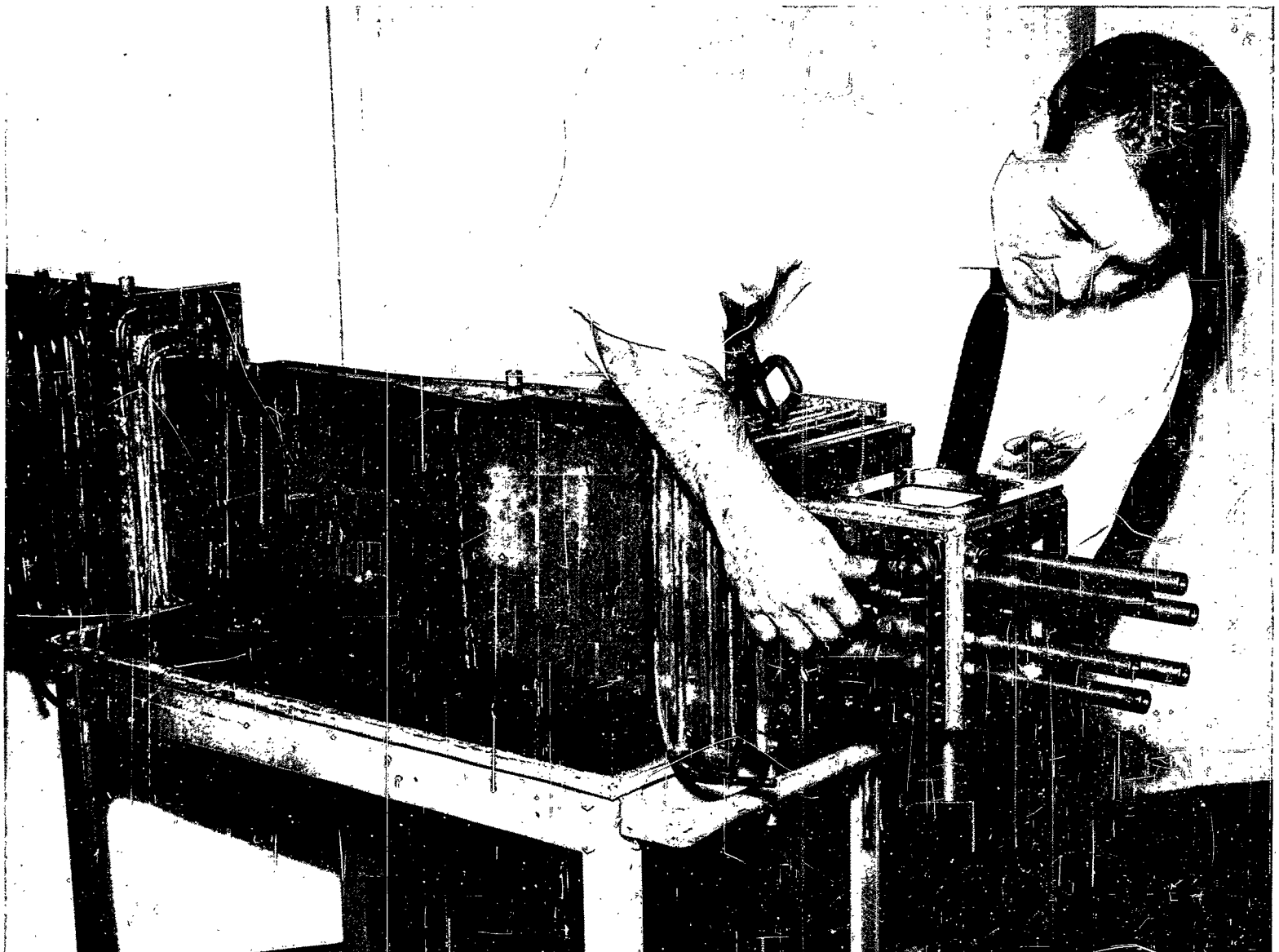

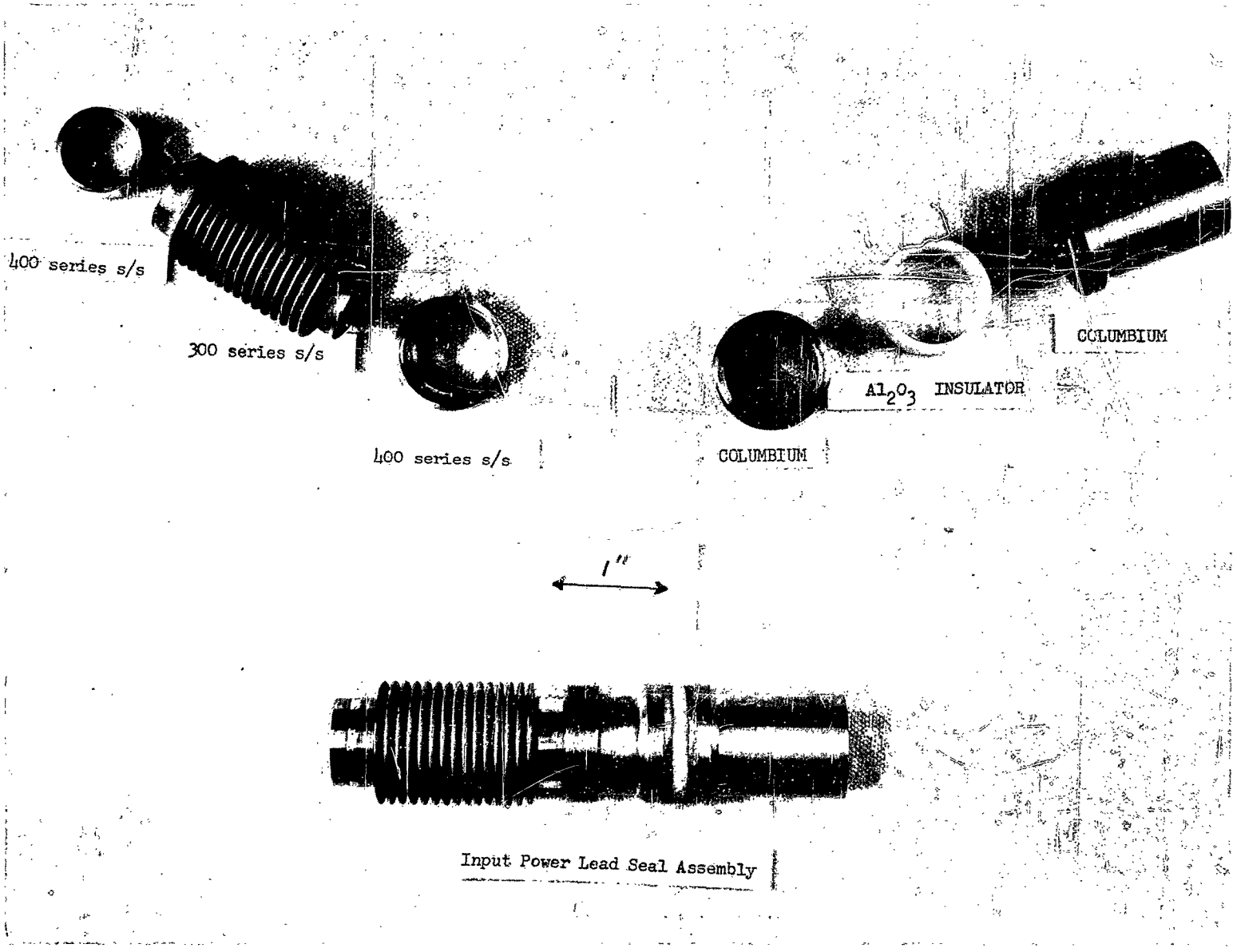

Input Power Lead Seal Assembly

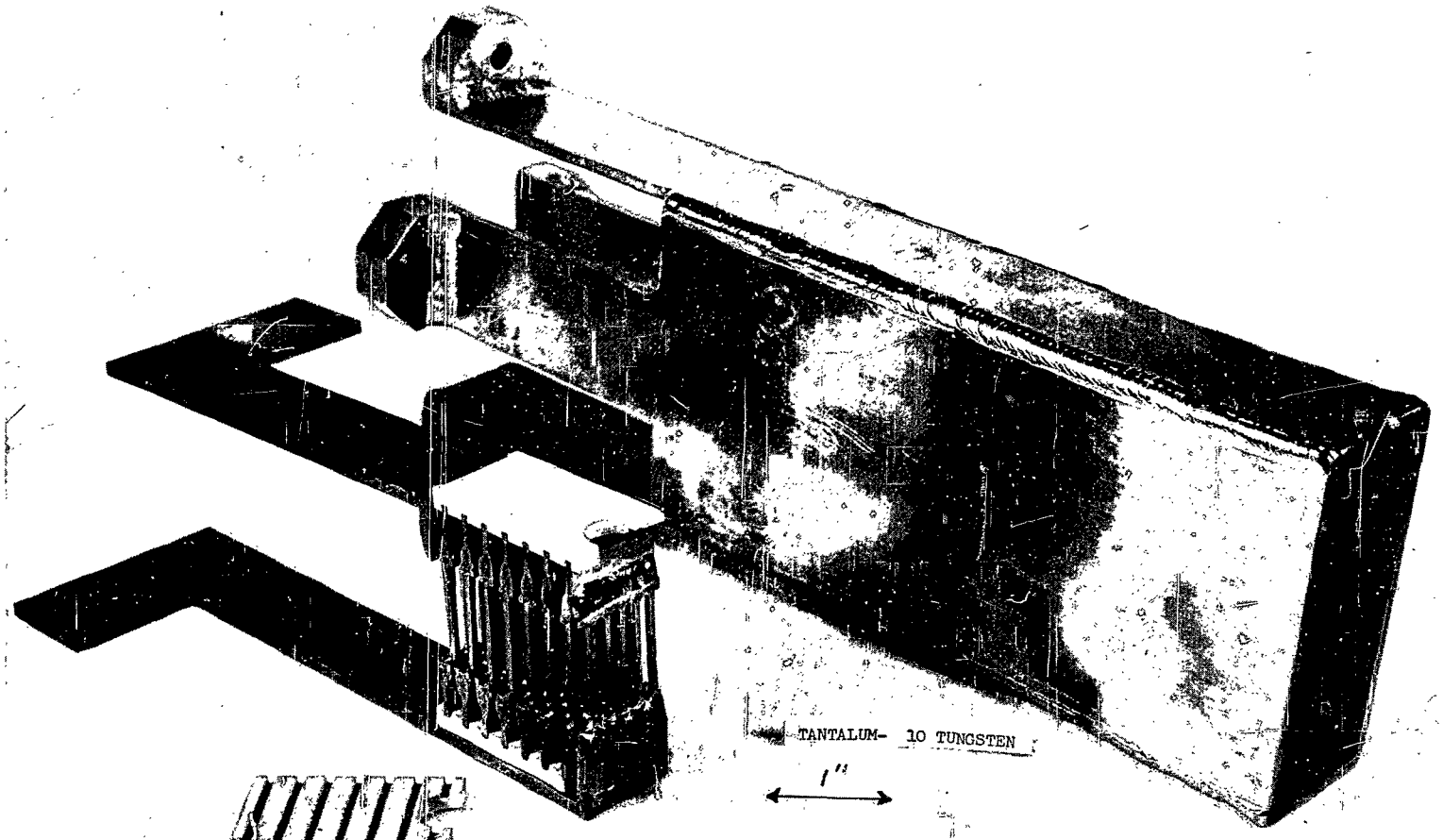

Heater Box and Element Assembly

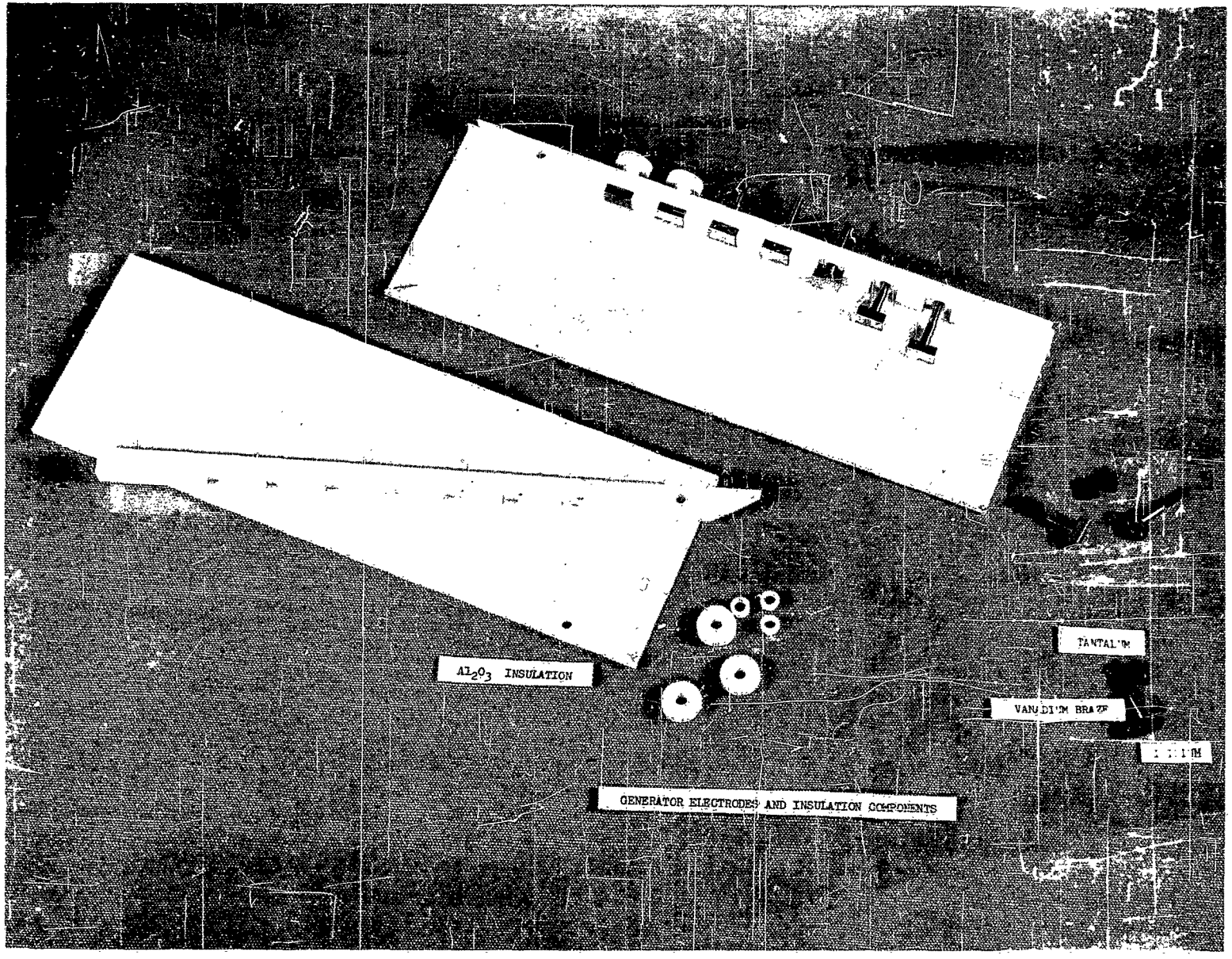
Al_2O_3 INSULATION
TANTALUM
VANADIUM BRAZE
GENERATOR ELECTRODES AND INSULATION COMPONENTS

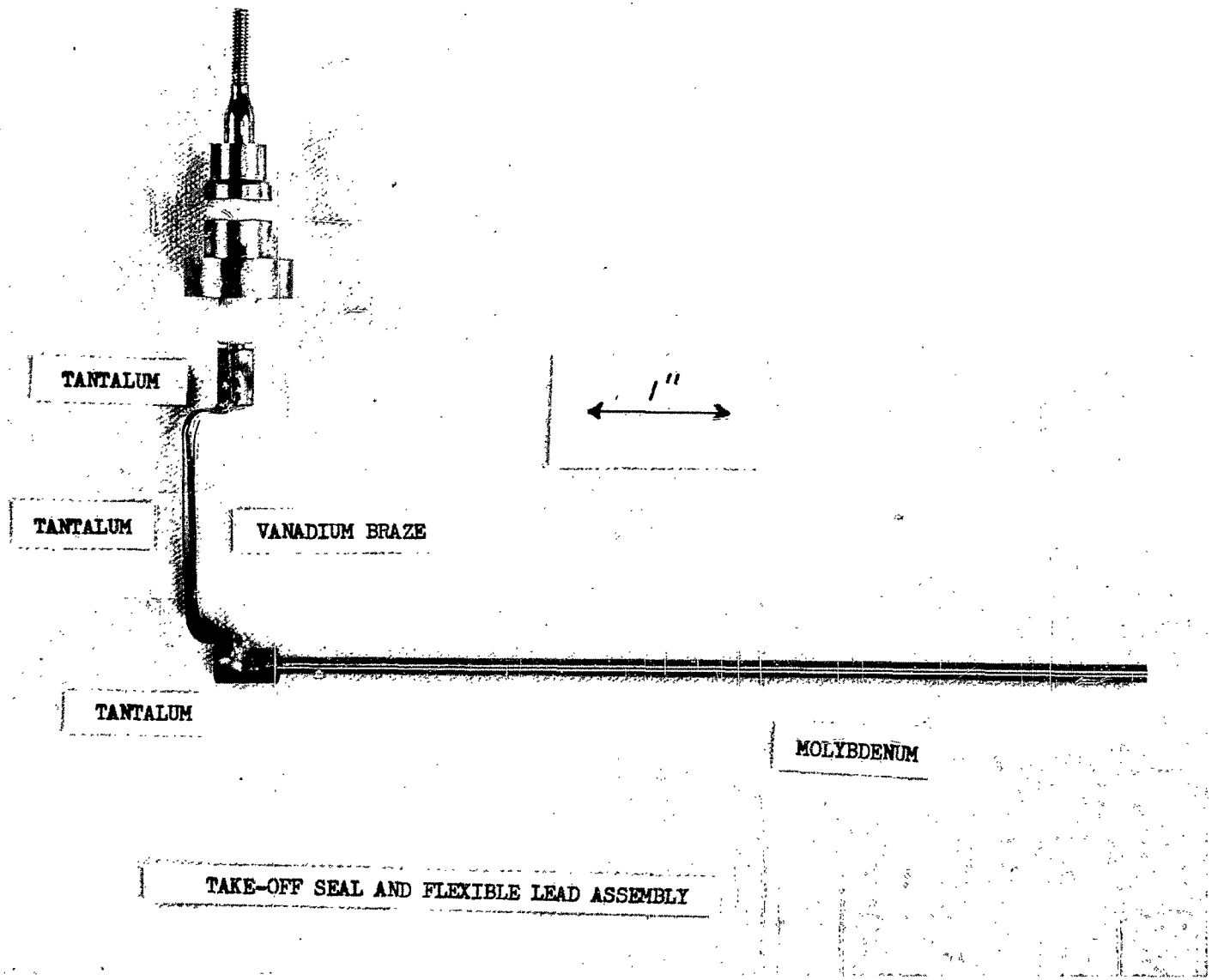

TAKE-OFF SEAL AND FLEXIBLE LEAD ASSEMBLY

IV. NON-EQUILIBRIUM IONIZATION STUDIES

This chapter is covered by the text of the following technical paper: "Comparison Between Test and Calculations of Non-Equilibrium Ionization Conductivities And the Corresponding Internal Electric Fields Required," presented at the Fourth Symposium on the Engineering Aspects of Magnetohydrodynamics held at Berkeley, California, April 11, 1963. Its text represents pages 11-17 of this report, and Figs. 1 to 4 of the paper represent Figs. 14 to 17 of this report.

COMPARISON BETWEEN TEST AND CALCULATIONS OF NON-EQUILIBRIUM IONIZATION CONDUCTIVITIES AND THE CORRESPONDING INTERNAL ELECTRIC FIELDS REQUIRED

M. E. Talaat
Martin Marietta Corporation, Baltimore 3, Maryland

INTRODUCTION

An ionized gas is said to be in the non-equilibrium state when the approximately Maxwellian electrons are maintained at a higher temperature than the Maxwellian ions and neutrals. When such a state exists in, for example, a seeded noble gas the ions could be primarily generated by ionizing collisions of the hot plasma electrons with the seed atoms and the gas temperature could be maintained at a sufficiently low value which is compatible with a nuclear reactor heat source. The term non-equilibrium ionization is used to refer to the ionization processes under these conditions. The realization of a practical closed loop magnetoplasmadynamic generator with a reactor heat source depends on the feasibility of attaining good electrical conductivities by application of the principles of non-equilibrium ionization to such a system.

Thus, it is important to be able to predict with close accuracy the electrical conductivity of an ionized gas in the non-equilibrium state and the corresponding electric field required for maintaining the hot plasma electrons and in turn the rate of generation of ions or ionization level which is necessary to yield that electrical conductivity. Accuracy in predicting the electrical conductivity is necessary because the output power density of a magnetoplasmadynamic generator is directly proportional to the conductivity, and accuracy in predicting the corresponding electric field required is necessary because it gives an indication of the feasibility of attaining the desired conductivity with non-equilibrium ionization under any given set of operating conditions.

In this paper we present a comparison between the calculated and measured values of the electrical conductivity and the corresponding electric fields required in a gas filled diode containing helium seeded with cesium. The calculations are based on the theory of non-equilibrium ionization which was developed in Reference 1, and in which the electron or ion density in the plasma is derived from an ion balance equation which equates the rate of generation of ions by the hot electrons in the plasma to the rate of loss of ions by recombination. The electric field required to maintain the hot electrons in the plasma is derived from an energy balance equation which equates the rate of energy lost by the electrons in elastic and inelastic collisions with the gas species to the rate of energy fed to the electrons through the electric field.

ENERGY BALANCE EQUATION

In the case of non-equilibrium ionization discussed in this paper, the rate of energy lost by the plasma electrons in ionizing, exciting and elastic collisions with the cesium seeded helium gas species is balanced by the rate of energy fed by the flow of a current density, I_e, under the electric field, $\mathcal{E}_e$. Thus,

$$I_e \mathcal{E}_e = P_{el} + P_{inel}$$

If the variation in the electrical conductivity of the plasma is negligible, the diffusion equation for electrons yields the following relation for the current density

$$I_e = \sigma \mathcal{E}_e$$

and the energy balance equation takes on the following form

$$\sigma \mathcal{E}_e^2 = P_{el} + P_{inel}$$

where for a Maxwellian distribution of electrons in a partially ionized cesium seeded helium gas we have (see Refs. 1 and 2)

$$P_{el} = 1.13 v_o n_g q_g \frac{8}{3}\frac{m_e}{m_g}\left(1 - \frac{E_g}{E_e}\right)\left[1 + 0.663\frac{m_g n_s q_{os}}{m_s n_g q_g} + 2.26\frac{m_g n_e q_p}{m_s n_g q_g}\right](1.5eE_e)n_e$$

$$P_{inel} = \left[\delta_i n_s e(V_i + 1.5E_e) + \delta_* n_s e V_*\right] n_e$$

$$\delta_i = 1.13 v_o (k\beta_i)(V_i + 2E_e)\exp - \frac{V_i}{E_e} \; ; \; (k\beta_i) = 0.79 \times 10^{-20} \text{ sq m/v (Von Engel 3)}$$

$$\delta_* = 1.13 v_o (k\beta_*)(V_* + 2E_e)\exp - \frac{V_i}{E_e}$$

$$\sigma = e n_e \frac{e}{m_e \gamma_c}$$

$$\gamma_c = v_o\left[1.33\, q_g n_g + q_{os} n_s + q_p n_e\right]$$

$q_g = (5.5)10^{-20}$ sq m for He

$q_{os} = (230)10^{-20}/\sqrt{E_e}$ sq m for Cs

$q_p = (248)10^{-20}(\ln \Lambda)/E_e^2$ sq m for ions

$\Lambda = (1.55)10^{13} E_e^{1.5}/n_e^{0.5}$

$E_e = (kT_e/e)$

$v_o = \left(\frac{2eE_e}{m_e}\right)^{0.5} = (0.593)10^6\sqrt{E_e}$ m/sec when E_e is in volts.

ELECTRIC FIELD

Next we substitute the expressions for P_{el}, P_{inel} and σ into the energy balance Eq. (3) and we obtain the following expression for the electric field, $\mathcal{E}_e$, inside the plasma which is required to maintain the flow of current and hence feed into the plasma the rate of energy necessary to maintain the approximately Maxwellian plasma electrons at any specific electron temperature E_e, namely,

$$\mathcal{E}_e = 2.12 n_g q_g E_e \sqrt{f}$$

where f is the equivalent average fraction of the electron energy which is lost in elastic and inelastic collisions and is given by (see Ref. 1)

$$f = \left[\frac{8m_e}{3m_g}\left(1 - \frac{E_g}{E_e}\right) \left\{ 1 + 0.663 \frac{m_g n_s q_{os}}{m_s n_g q_g} + 2.26 \frac{m_g n_e q_p}{m_s n_g q_g} \right\} + 0.59 \frac{n_s}{n_g} \frac{\delta_i}{v_o q_g} \left(\frac{V_i}{E_e} + 1.5\right) \left\{ 1 + \frac{V_*}{V_i + 1.5E_e} \frac{\beta_*}{\beta_i} \frac{V_* + 2E_e}{V_i + 2E_e} \exp \frac{V_i - V_*}{E_e} \right\} \right] \left\{ 1 + 0.752 \frac{n_s q_{os} + n_e q_p}{n_g q_p} \right\}$$

ELECTRON DENSITY

The electron density, n_e, appearing in the expression for the electric field, $\mathcal{E}_e$, and in the expression for the electrical conductivity, σ, is a function of the electron temperature and is derived from the generalized differential expression of the ion balance equation which equates the rate of generation of ions, ν_i, to the rate of loss of ions by diffusion $\frac{1}{e} \nabla \cdot \Gamma_p$ and by volume recombination $\alpha_r n_e n_p$, namely,

$$e \nu_i = \nabla \cdot \Gamma_p + e \alpha_r n_e n_p$$

Now if the conditions are such that the diffusion to the walls is negligible by comparison to volume recombination and if the gas temperature, E_g, is low by comparison to the electron temperature, E_e, such that the only important mechanism of ionization (see Ref. 1) is by collision of the hot electrons with the seed atoms (viz., the rate of generation of ions $\nu_i = \delta_i n_s n_e$) then the ion balance equation yields the following approximate equation for the electron density

$$n_e \approx \frac{\delta_i}{\delta_i + \alpha_r} n_{so}$$

where the recombination coefficient, α_r, has in most cases of interest as the dominant component the Thomson 3 body recombination coefficient, α_T, namely (see Ref. 1)

$$\alpha_r \approx \alpha_T = (2.68)10^{-21} E_e^{-2.5} n_g q_g \left\{1 + 0.752 \frac{n_s q_{os} + n_e q_p}{n_g q_g}\right\} f$$

RESULTS

The electrical conductivity and the electric field versus current density curves for any given case of seeded noble gas can now be computed by solving these equations for the electron density, the corresponding electrical conductivity, the corresponding electric field and the corresponding current density at several chosen values of the electron temperature, E_e.

The results of the calculations are presented in Figs. 1 and 3 for the case of a helium gas density of 1.61×10^{24} atoms/m^3 seeded with a cesium seed density of 0.818×10^{22} atoms/m^3 (corresponding to a liquid cesium temperature of 523°K or 0.045 volt). In one set of calculations the gas temperature is taken to be the same as the temperature of the electrodes in the diode tube, viz., $E_g = 0.144$ volt (corresponding to a temperature of the electrodes = 1670°K)(see Fig. 1) while in another set of calculations the gas temperature is taken to be the same as the

liquid cesium temperature, viz., E_g = .045 volt (see Fig. 3). The solid lines are based on a value for the initial slope of the ionization cross section curve for cesium derived from Von Engel $k\rho_i = 0.79 \times 10^{-20}$ sq m/volt and with an assumed equal value for the initial slope of the excitation cross section curve for cesium. The dashed curves are based on a value of the initial slope of the ionization cross section curve for cesium = 10 times that used in deriving the solid curves, but with the initial slope of the excitation cross section curve equal to that used in deriving the solid curves.

The experimental points indicated in Fig. 1 were obtained from tests on a 0.0135 meter long diode tube with hot electrodes and filled with the cesium-seeded helium. These points were evaluated from the voltage-current density curve shown in Fig. 2 (taken from Fig. 27 of Reference 4) with the electrodes maintained at a temperature of 1670°K.

The experimental points indicated in Fig. 3 were obtained from tests on a 0.23 meter long diode tube with hot electrodes and filled with the cesium-seeded helium. These points were evaluated from voltage and current readings at a time of about 25-50 micro sec after the initiation of the discharge which was long with respect to the time required for collisional ionization equilibrium, but short with respect to the time for heating the gas. Thus, all experimental points for this figure can be considered to have been obtained at approximately the same steady-state gas temperature of 523°K.

It is seen that the agreement between the theoretical and experimental results is very good. The calculated values of electric fields required to maintain a certain current density are generally higher than those measured in the experiment for current densities in the range of about 1 to about 20 amps per sq cm. The positive resistance characteristic predicted by the theory is also verified by the experimental results. The calculated solid curve values of the corresponding electrical conductivities are lower than those measured.

Since these calculations are based on values of electron densities which are computed using the ion balance equation rather than those which would be obtained from using the electron temperature in Saha's equation for thermal ionization, it is of interest to compare plots of the calculated electrical conductivities versus electron temperature using the two approaches in obtaining the electron densities. In Fig. 4 the dotted curve was derived using the electron density from Saha's equilibrium equation with the electron temperature inserted. The solid and dashed curves were derived for E_g = 0.045 volt using the electron density as obtained from the ion balance equation with the value of the initial slope of the ionization cross section in the dashed curve taken to be equal to ten times the value given in Von Engel's book on Ionized Gases and which was used in deriving the solid curve. It is seen that the curve using the electron density from Saha's equation with E_e inserted gives higher values of electrical conductivities (sometimes by more than two orders of magnitude) than both curves using the electron density from the ion balance equation with an ionization cross section of cesium as given by Von Engel or with ten times that value.

CONCLUSION

In conclusion, the comparison between test and calculations based on a theory of non-equilibrium ionization (Ref. 1) in which the electron density is derived from an ion balance equation and the electric field is derived from an energy balance equation indicates very good agreement between experiment and theory. Both theoretical calculations and experimental results obtained in the diode tubes filled with helium seeded with about 0.5% cesium and helium density of 1.61×10^{24} atoms/m^3 show that electrical conductivities on the order of 100 mho/m are obtained at current densities on the order of 10×10^4 amp/sq m and with an electric field on the order of 1200 volt/m. These values are of interest in MPD electrical power generation with non-equilibrium ionization.

REFERENCES

1. Talaat, M. E., "Magnetoplasmadynamic Electric Power Generation With Non-Equilibrium Ionization," Paper presented September 6, 1962 before the Symposium on Magnetoplasmadynamic Electrical Power Generation held at King's College, University of Durham, Newcastle Upon Tyne, England.

2. Talaat, M. E., "Generalized Theory of the Thermionic Plasma Energy Converter," AIEE Transaction Paper 62-291.

3. Von Engel, A., "Ionized Gases," Oxford Press, London, 1955.

4. Martin Company Semi-Annual Technical Summary Report (June 15 - December 15, 1962), MND-2939,"Research Program on Closed-Cycle MPD Electrical Power Generation With Non-Equilibrium Ionization."

$n_{s_0} = 0.818 \times 10^{22}/m^3$ (Cs)

$n_g = 1.61 \times 10^{24}/m^3$ (Hg)

$E_g = 0.144$ VOLT

σ (MHO/METER) OR
$\mathcal{E}_e$ (10^2 VOLTS/METER)

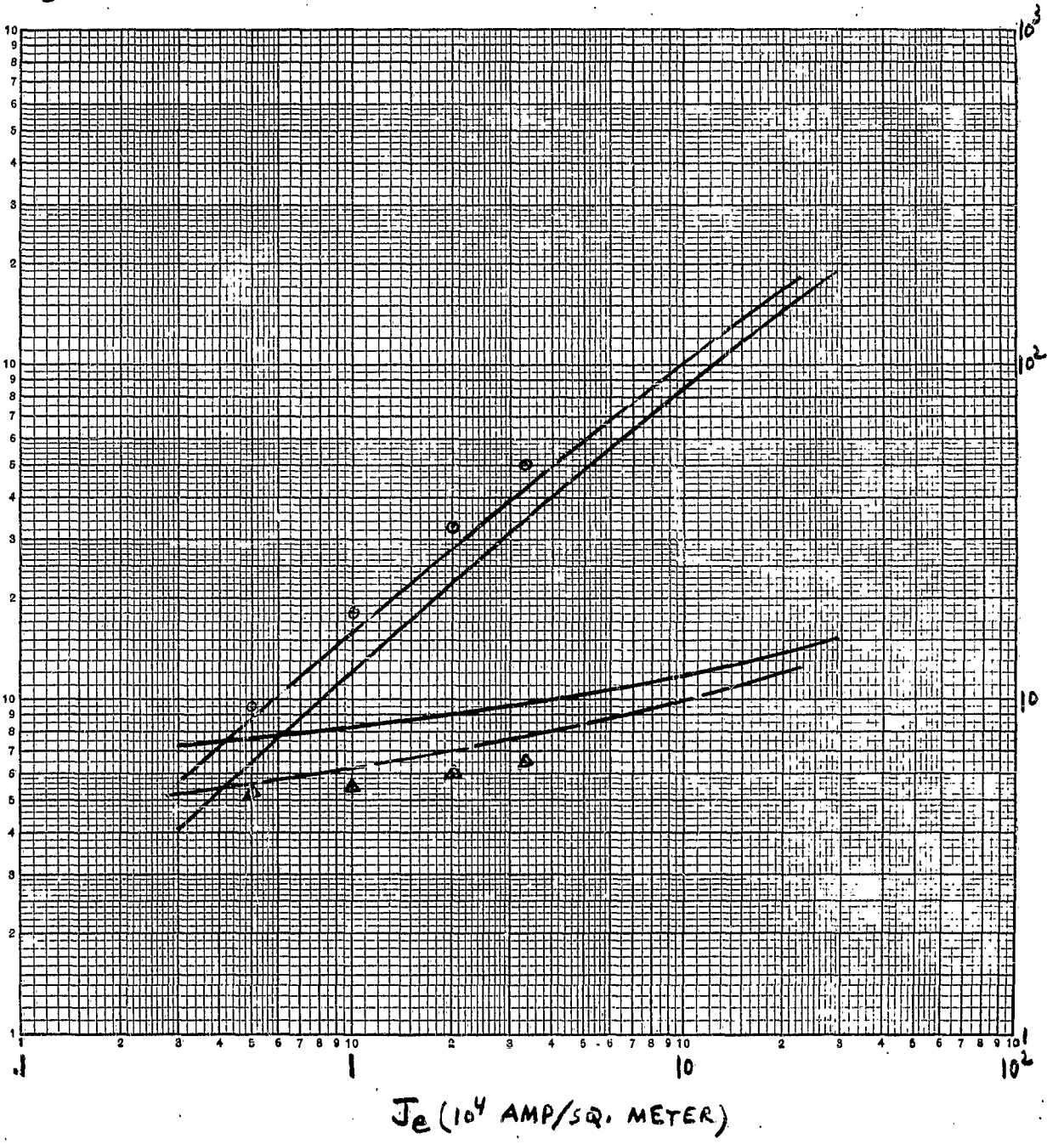

Fig. 1 MET

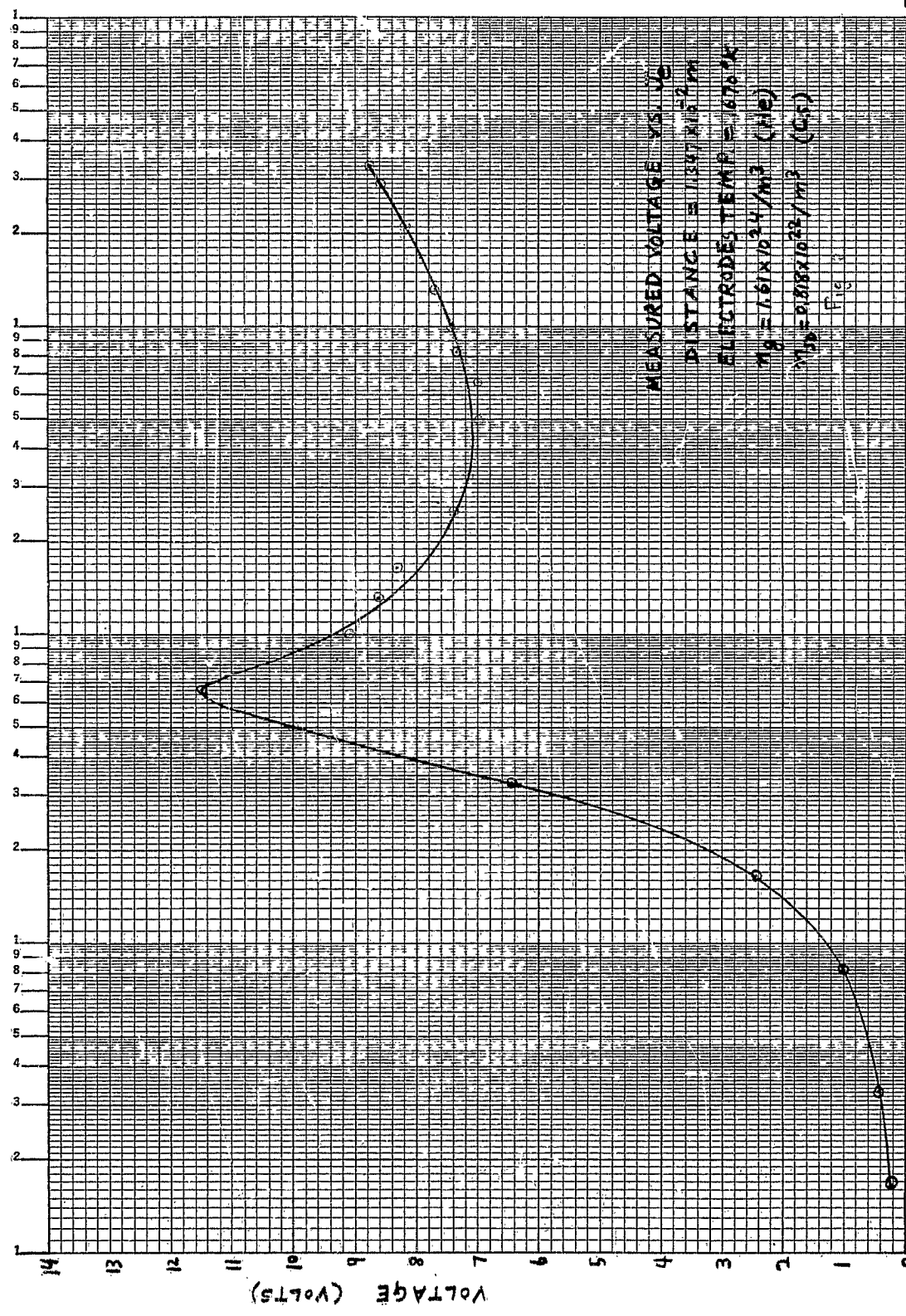
MEASURED VOLTAGE VS. J_e
DISTANCE = 1.397×10^{-2} m
ELECTRODES TEMP = 670 °K
$n_e = 1.61 \times 10^{24}$ /m^3 (He)
$n_p = 0.808 \times 10^{22}$ /m^3 (Cs$^+$)
FIG. 3
VOLTAGE (VOLTS)
J_e (AMPS/SQ.M) CURRENT DENSITY
10^2
10^3
10^4
10^5

$n_{s_0} = 0.818 \times 10^{22} / M^3$ (Cs)

$n_g = 1.61 \times 10^{24} / M^3$ (He)

$E_g = 0.045$ VOLT

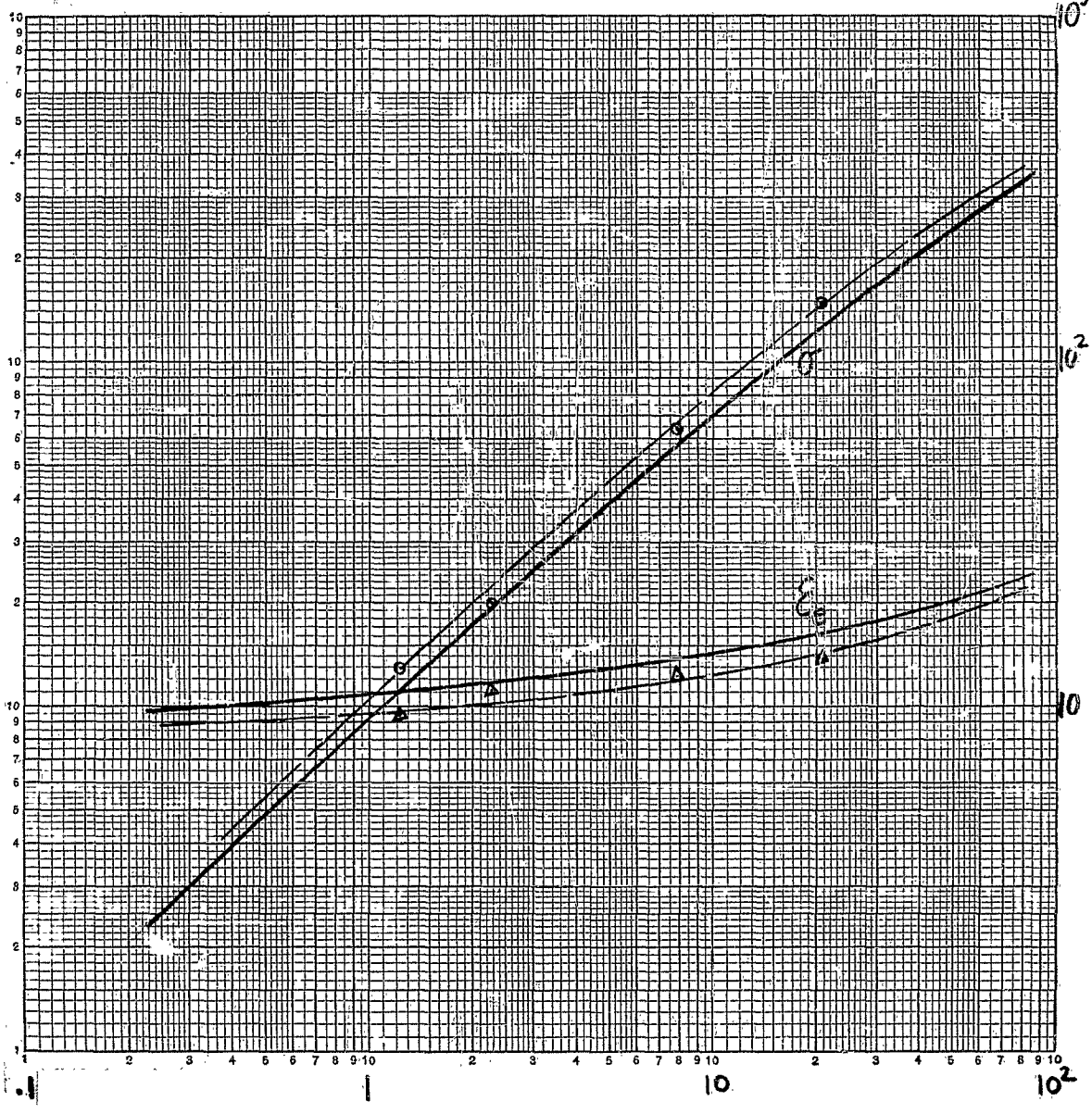

Fig. 3

MET

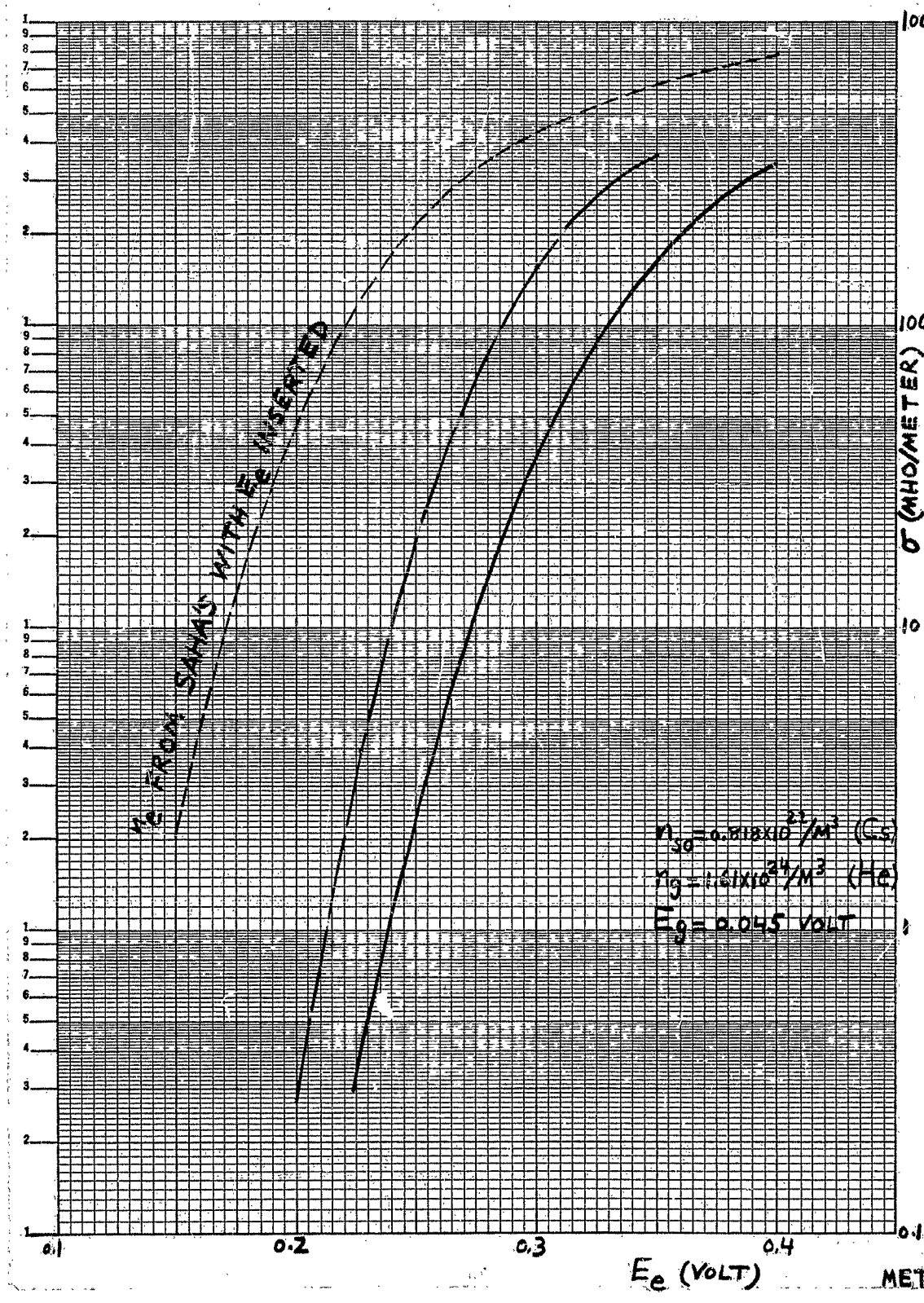
1000
100
10
1
0.1
σ (MHO/METER)
0.1
0.2
0.3
0.4
E_e (VOLT)
MET
SAHA'S WITH E_g INSERTED
$n_{so} = 0.818 \times 10^{23}/M^3$ (Cs)
$n_g = 1.61 \times 10^{24}/M^3$ (He)
$E_g = 0.045$ VOLT

V. STUDY AND ANALYSIS OF CLOSED-CYCLE MPD POWER GENERATION UNDER CONDITIONS COMPATIBLE WITH NON-EQUILIBRIUM IONIZATION

1. Introduction

In the following articles and subsequent articles in future reports under this title we will analyze the operation of the closed-cycle MPD power generator under conditions which are compatible with attaining the electrical conductivity in the MPD duct by means of non-equilibrium ionization techniques (either by magnetically induced electron heating or by other auxiliary ionization techniques such as photoionization, electron injection gun, auxiliary d-c, a-c or h.f. discharge, etc.). We will, first, in the following sections, obtain solutions of the MPD power generator equations for the following cases:

a. Constant velocity segmented electrodes Faraday generator with constant electrical conductivity, σ_0, and constant internal voltage drop between each electrode pair along the duct (i.e. constant current density flow between each electrode pair along the duct).

b. Constant area duct segmented electrodes Faraday generator with constant electrical conductivity, σ_0, and constant internal voltage drop between each electrode pair along the duct (i.e. constant current density flow between each electrode pair along the duct).

c. Constant area duct segmented electrodes Faraday generator with constant electrical conductivity, σ_0, and constant electrical load resistance for each electrode pair along the duct.

d. Constant area duct segmented electrodes Faraday generator with constant electrical conductivity, σ_0, and constant output voltage along the duct.

The solutions (e.g. power density, efficiency and duct length) are presented here in figures using universal dimensionless factors which can be used in the analysis or design of any generator of the types specified in cases (a) to (d).

In subsequent articles in future reports under this title we will examine the solution of the MPD power generation equations for the case of segmented electrodes Hall generator and under conditions similar to those listed in (a) to (d).

These solutions will be used to evaluate the MPD power generation cycle in which the reject heat from the MPD generator duct is used to power the compressor necessary for closing the cycle. In this context we will evaluate and assess the use of the jet compressor as well as the conventional mechanical compressor. We will also present the basic equations governing the behavior of the simple constant area mixing jet compressor.

Examples of calculations will be selected and numerical evaluations of the performance of typical generator and its suitable compressor will be carried out.

2. General Equations of the MPD Power Generator

The equations governing the behavior of the MPD electric power generator[1] are Maxwell's electromagnetic field equations, the generalized Ohm's law and the gas dynamic equations modified to take account of the interaction between the motion and the magnetic field and the energy equation.

Maxwell's Equations:

Maxwell's equations consist essentially of the following:

a. The generalized differential expression of Faraday's law for the curl of the electric field, viz.,

$$\nabla \times \underline{E} = -\frac{\partial \underline{B}}{\partial t} \tag{1}$$

b. The generalized differential expression of Gauss' law for the divergence of the magnetic field, viz.,

$$\nabla \cdot \underline{B} = 0 \tag{2}$$

c. The generalized differential expression of Biot and Savart's law for the curl of the magnetic field, viz.,

$$\nabla \times \underline{B} = \mu \cdot \underline{J} + \mu_o \epsilon_o \frac{\partial \underline{E}}{\partial t} \tag{3}$$

d. The generalized differential expression of Gauss' law for the divergence of the electric field, viz.,

$$\nabla \cdot \underline{E} = (\rho_q / \epsilon_o) \qquad \text{(Poisson's Equation)} \tag{4}$$

---

1. Talaat, M. E., "Magnetohydrodynamic Electric Power Generators," Advanced Energy Conversion, Vol. 1, pp. 19-35, Pergamon Press, 1961.

Ohm's Law

The generalized differential expression of Ohm's law[2] for a moving medium includes beside the term due to the electric field, $\underline{\mathcal{E}}$, a term due to the induced electric field, $(\underline{u} - \frac{\underline{J}}{en_e}) \times \underline{B}$, resulting from the motion of the medium at velocity, $\underline{u}$, under the influence of the magnetic field intensity, $\underline{B}$, a term due to the transport of the net charge density, ρ_q, by the medium moving with a velocity, $\underline{u}$, and a term due to the electron pressure gradient $\nabla p_e = \nabla(n_e kT_e)$

$$\underline{J} = \sigma \left[\underline{\mathcal{E}} + (\underline{u} - \frac{\underline{J}}{en_e}) \times \underline{B} + \frac{1}{en_e} \nabla p_e \right] + \rho_q \underline{u} \qquad (5)$$

Note that if $\underline{u} = 0$ and $\underline{B} = 0$ then

$$\underline{J} = \sigma \underline{\mathcal{E}} + \frac{\sigma}{en_e} \nabla p_e = en_e \mu_e \underline{\mathcal{E}} + \mu_e \nabla (n_e kT_e) = en_e \mu_e \underline{\mathcal{E}} + \nabla (en_e \mathcal{E}_e \mu_e) \qquad (5a)$$

which is the diffusion equation of electrons under no magnetic field[3].

When $\underline{u} = 0$ and $\underline{B} \neq 0$ then

$$\underline{J} = \sigma \underline{\mathcal{E}} + \mu_e \nabla (n_e kT_e) - \frac{1}{en_e} \underline{J} \times \underline{B} \qquad (5b)$$

which is the diffusion equation of electrons in a magnetic field.

Gas Dynamic Equations

The gas dynamic equations consist of the following:

a. The differential expression of the mass continuity equation

$$\frac{\partial \rho}{\partial t} + \nabla \cdot (\rho \underline{u}) = 0 \rightarrow \frac{\partial (\rho A)}{\partial t} + \nabla \cdot (\rho A \underline{u}) = 0 \quad \text{(for variable area A)} \qquad (6)$$

2. Spitzer, L., Physics of Fully Ionized Gases
3. Allis, W. P., "Motion of Ions and Electrons," Handbuch der Physik, Vol. XXI, p. 397, Eq. 15.3, Springer-Verlag, 1956.

b. The differential equation of motion which is essentially a statement of Newton's second law for a differential volume of the moving medium

$$\rho\left[\frac{\partial \underline{u}}{\partial t} + (\underline{u}\cdot\nabla)\,\underline{u}\right] = -\nabla p + \underline{J}\times\underline{B} + \rho_q\underline{\mathcal{E}} + \rho g + \rho\nu\nabla^2 u + (1/3)\,\rho\nu\nabla(\nabla\cdot\underline{u}) \tag{7}$$

Energy Equation

The differential equation for the generalized energy equation for a compressible fluid flow has in addition to the internal energy term

$$\rho\left[\frac{\partial U}{\partial t} + \underline{u}\cdot\nabla\, U\right]$$

where $U = \int C_v dT$, and the term representing the work done by motion

$$\frac{p}{\rho}\left[\frac{\partial \rho}{\partial t} + \underline{u}\cdot\nabla\rho\right]$$

heat terms per unit volume due to Joule heat $\frac{1}{\sigma}J^2$, due to heat conduction $k\nabla^2 T$ and due to viscosity $\left\{\frac{1}{2}\rho\nu\left[\nabla\underline{u} + (\nabla\underline{u})_*\right]^2\right\}$

Thus

$$\rho\left[\frac{\partial U}{\partial t} + \underline{u}\cdot\nabla U\right] = \frac{p}{\rho}\left[\frac{\partial \rho}{\partial t} + \underline{u}\cdot\nabla\rho\right] + \frac{1}{\sigma}J^2 + k\nabla^2 T + \frac{1}{2}\rho\nu\left[\nabla\underline{u} + (\nabla\underline{u})_*\right]^2 \tag{8}$$

where the asterisk denotes the transpose of the tensor.

3. MPD Power Generator Steady-State One-Dimensional Flow Equations

By applying the following conditions and assumptions to the generalized equations governing the behavior of the MPD power generator, these equations take on scalar forms which can be readily solved.

a. The operation of the generator is in the steady-state (i.e. $\frac{\partial}{\partial t} = 0$)

b. The gas flow is strictly one dimensional which means that all variables, in addition to the gas dynamical variables, vary only in the direction of flow (x-direction), but not over the cross section of the channel

c. The applied magnetic field is in the z-direction and is constant (i.e. $B_z = B$)

d. The current flow is possible in the x and y directions only (i.e. $J_z = 0$)

e. The electrical conductivity, σ_o, of the ionized gas is constant (i.e. $\sigma_o = e(n_e\mu_e + n_p\mu_p)$)

f. The electron pressure gradient of the ionized gas is zero, i.e. $\nabla p_e = \nabla(kT_e n_e) = 0$

g. The ionized gas is electrically neutral (i.e. $n_e = n_p$)

h. The effects of gravity, viscosity or thermal conductivity of the gas can be neglected

i. The ionized gas or plasma obeys the perfect gas law (i.e. $p = \rho RT$)

j. The ratio, γ, of specific heat at constant pressure to specific heat at constant volume of the gas is constant

k. The ionized gas flow through the generator duct is free from shocks, i.e. the flow is free from any regions in which the temperature, pressure or density change very rapidly with distance

l. The voltage drops at the electrode sheaths are small in comparison with the generated voltage and can be neglected.

Thus the generalized equations governing the behavior of the MPD power generator can be reduced to the following scalar forms:

a. Ohm's Law (neglecting electron pressure gradients and ion slip)

1) The current density, J_x, in the direction of flow is given by

$$J_x = \frac{\sigma_o}{1+\beta^2}\left[\mathcal{E}_x - \beta(\mathcal{E}_y - uB)\right] \tag{9}$$

2) The current density, J_y, across the interelectrode spacing (perpendicular to the direction of flow and perpendicular to the magnetic field)

$$J_y = \frac{\sigma_o}{1+\beta^2}\left[\beta\mathcal{E}_x + (\mathcal{E}_y - uB)\right] \tag{10}$$

where

$$\beta = \omega t = \mu_e B \tag{11}$$

b. Gasdynamic Equations

1) Continuity Equation

$$\frac{d}{dx}(\rho uA) = 0 \tag{12}$$

$$puA = \rho_o u_o A_o = \text{constant} \tag{13}$$

2) Equation of Motion

$$\rho u\frac{du}{dx} + \frac{dp}{dx} = J_y B \tag{14}$$

c. Energy Equation

$$\rho u\frac{dU}{dx} = \frac{p}{\rho} u\frac{d\rho}{dx} + \frac{1}{\sigma_o} J^2 \tag{15}$$

where

$$U = C_v T \quad \text{and} \tag{16}$$

$$J^2 = J_x^2 + J_y^2 \tag{17}$$

d. Equation of State

$$p = \rho RT = \rho \frac{R_o}{Z} T \tag{18}$$

where $R_o = 8.314$ Joules/°K is the universal gas constant and Z is the atomic weight in Kg(e.g. $Z = 0.004$ Kg for He).

Differentiating the equation of state (18) with respect to x and then substituting $\frac{d\rho}{dx}$ into the energy equation (15) we get the following expression

$$\rho u \frac{d}{dx}(C_V + R)T = u \frac{dp}{dx} + \frac{1}{\sigma_o} J^2 \tag{19}$$

By substituting for $\frac{dp}{dx}$ from the equation of motion (14) into the energy equation (19) and since $C_p = C_V + R$ we get, after rearranging terms, the following expression for the energy equation

$$\rho u \frac{d}{dx}(C_p T + \frac{1}{2} u^2) = uBJ_y + \frac{1}{\sigma_o} J^2$$

$$= (uB + \frac{1}{\sigma_o} J_y) J_y + \frac{1}{\sigma_o} J_x^2 \tag{20}$$

A. Solution For the Constant Velocity Case

In this case $u = u_o$ = constant and the MPD power generator gas dynamic and energy equations reduce to the following simple form:

a. Continuity Equation

$$\rho A = \rho_o A_o = \text{constant} = \rho_o G_o D_o = \rho G D_o \tag{21}$$

b. Equation of Motion

$$\frac{dp}{dx} = J_y B \tag{22}$$

c. Energy Equation

$$\rho u \frac{d}{dx}(C_p T) = (uB + \frac{1}{\sigma_o} J_y) J_y + \frac{1}{\sigma_o} J_x^2 \tag{23}$$

1) Segmented Electrodes Faraday Generator

In this case $J_x = 0$ and solution for the electric field in the x direction from equation (9) yields the following expression for $\mathcal{E}_x$

$$\mathcal{E}_x = \beta(\mathcal{E}_y - uB) \tag{24}$$

Substituting this value of $\mathcal{E}_x$ into the expression for J_y (Eq. 10) we get the following expression

$$J_y = \sigma_o(\mathcal{E}_y - uB) \tag{25}$$

which for an electric load factor

$$e_L = \frac{V}{V_{oc}} = \frac{\text{load voltage}}{\text{open circuit voltage}} = \frac{\mathcal{E}_y D_o}{uBD_o} \tag{26}$$

can be written as follows

$$J_y = -\sigma_o uB(1 - e_L) = \text{constant for constant } \sigma_o . \tag{27}$$

Substituting this equation (27) for J_y in the equation of motion (22) we get

$$\frac{dp}{dx} = -u\sigma_o B^2(1 - e_L) \tag{28}$$

Solution of equation (28) gives for the pressure, p, at any distant x the following expression

$$p = p_o - u\sigma_o B^2(1 - e_L)x \tag{29}$$

Now from the equation of state and the definition of Mach number, M (viz., $u^2 = M^2 \gamma RT$), we can derive the following expression for the

density, ρ , in terms of the velocity, u, the pressure, p, and the Mach number, M, namely

$$\rho = \frac{\gamma M^2 p}{u^2} \tag{30}$$

By substituting into the energy equation (23) the expression for ρ given by equation (30), the expression for J_y given by equation (27) and the relation $C_p T = \frac{\gamma}{\gamma - 1} RT = \frac{u^2}{(\gamma - 1)M^2}$ and then rearranging terms, we obtain the following differential equation for the Mach number, M, namely

$$\frac{dM}{M} = \frac{\alpha}{2} \frac{u \sigma_o B^2 (1 - e_L) dx}{p_o - u \sigma_o B^2 (1 - e_L) x} \tag{31}$$

Solution of this differential equation gives for the Mach number, M, at any distant, x, the following expression

$$\ln \frac{M}{M_o} = -\frac{\alpha}{2} \ln \frac{p_o - u \sigma_o B^2 (1 - e_L) x}{p_o} = \frac{\alpha}{2} \ln \frac{p_o}{p_o - u \sigma_o B^2 (1 - e_L) x} \tag{32}$$

where M_o is the Mach number at the entrance to the magnetic field-current interaction region. Thus the Mach number at any distance, x, is given by

$$\frac{M}{M_o} = \left[\frac{p_o}{p_o - u \sigma_o B^2 (1 - e_L) x} \right]^{\alpha/2} = \left(\frac{p_o}{p} \right)^{\alpha/2} \tag{33}$$

where

$$\alpha = (\gamma - 1) e_L / \gamma \tag{34}$$

The gas density, ρ , can now be given by substituting the relation between p and M given by equation (33) into equation (30). Hence,

$$\rho = \frac{\gamma M_o^2}{u^2} \left(\frac{p_o}{p} \right)^{\alpha} p = \frac{\gamma M_o^2 p_o}{u^2} \left(\frac{p_o}{p} \right)^{\alpha - 1} = \rho_o \left(\frac{p}{p_o} \right)^{1 - \alpha} = \rho_o \left(\frac{M_o}{M} \right)^{2(1 - \alpha)/\alpha} \tag{35}$$

Now from the continuity equation (21) the dimension G of the duct must be varied according to the following equation

$$G = G_o \frac{\rho_o}{\rho} = G_o \left(\frac{M}{M_o} \right)^{2(1-\alpha)/\alpha} = G_o \left(\frac{p_o}{p} \right)^{(1-\alpha)} = G_o \left(\frac{p}{p_o} \right)^{(\alpha - 1)}$$

or

$$\frac{G}{G_o} = \left(\frac{p_o}{p} \right)^{1-\alpha} = \left(\frac{M}{M_o} \right)^{2(1-\alpha)/\alpha} \tag{36}$$

The power output is given by the following integral

$$W_e = \int_0^L J_y \mathcal{E}_y \, DG dx \tag{37}$$

Substituting for J_y from equation (27), for $\mathcal{E}_y$ the expression uBe_L, for G from equation (36) and for dx from equation (28) we get the following integral

$$W_e = \int_{p_o}^{p_o} ue_L D_o G_o p_o \left(\frac{p}{p_o} \right)^{(\alpha - 1)} d\left(\frac{p}{p_o} \right)$$

$$= - \frac{\gamma}{\gamma - 1} p_o u D_o G_o \left[1 - \left(\frac{p}{p_o} \right)^{\alpha} \right]$$

$$= - \frac{\gamma}{\gamma - 1} p_o u D_o G_o \left[1 - \left(\frac{M_o}{M} \right)^2 \right] \tag{38}$$

Now the generator volume is given by the integral

$$\int_0^L DG dx = \int_{p_o}^{p} D_o G_o \left(\frac{p}{p_o} \right)^{(\alpha - 1)} \left[\frac{dp}{-u \sigma_o B^2 (1 - e_L)} \right] \tag{39}$$

$$= D_o G_o p_o \frac{\gamma}{\gamma - 1} \left[1 - \left(\frac{p}{p_o} \right)^{\alpha} \right] \frac{1}{u \sigma_o B^2 (1 - e_L) e_L}$$

Dividing the total output power by the volume, we get the following expression for the average output power density

$$w_e = - u^2 \sigma_o B^2 e_L (1 - e_L) \tag{40}$$

and since $u_o^2 = M_o^2 \gamma RT_o$ and $T_o = \dfrac{T_{So}}{1 + \dfrac{\gamma - 1}{2} M_o^2}$, hence,

$$w_e = - M_o^2 \gamma RT_o \sigma_o B^2 e_L (1 - e_L)$$

$$= - \gamma \frac{R_o}{z} T_{So} \frac{M_o^2}{1 + \dfrac{\gamma - 1}{2} M_o^2} \sigma_o B^2 e_L (1 - e_L)$$

$$= - \left(\frac{\gamma}{\gamma - 1} \frac{R_o}{z}\right) T_{So} \sigma_o B^2 \frac{(\gamma - 1) M_o^2}{1 + \dfrac{\gamma - 1}{2} M_o^2} e_L (1 - e_L) \tag{41}$$

or

$$\frac{w_e}{C_p T_{So} \sigma B^2} = \frac{(\gamma - 1) M_o^2}{1 + \dfrac{\gamma - 1}{2} M_o^2} e_L (1 - e_L) \tag{41a}$$

The inlet power is given by

$$W_o = \rho_o u A_o C_p T_{So} = u D_o G_o \rho_o RT_o \frac{\gamma}{\gamma - 1} \left(1 + \frac{\gamma - 1}{2} M_o^2\right) = D_o G_o \rho_o u \left[\frac{u^2}{(\gamma - 1) M_o^2} + \frac{1}{2} u^2\right]$$

$$= \frac{\gamma}{\gamma - 1} p_o u D_o G_o \left(1 + \frac{\gamma - 1}{2} M_o^2\right) \tag{42}$$

Hence the power conversion efficiency is given by

$$\eta = \frac{-W_e}{W_o} = \frac{1 - \left(\dfrac{p_r}{p_o}\right)^{\alpha}}{1 + \dfrac{\gamma - 1}{2} M_o^2} = \frac{1 - \left(\dfrac{M_o}{M_r}\right)^2}{1 + \dfrac{\gamma - 1}{2} M_o^2} \tag{43}$$

since from equation (33) we have

$$\frac{p_r}{p_o} = 1 - \frac{u \sigma_o B^2 (1 - e_L) L}{p_o} = \left(\frac{M_o}{M_r}\right)^{2/\alpha} \tag{44}$$

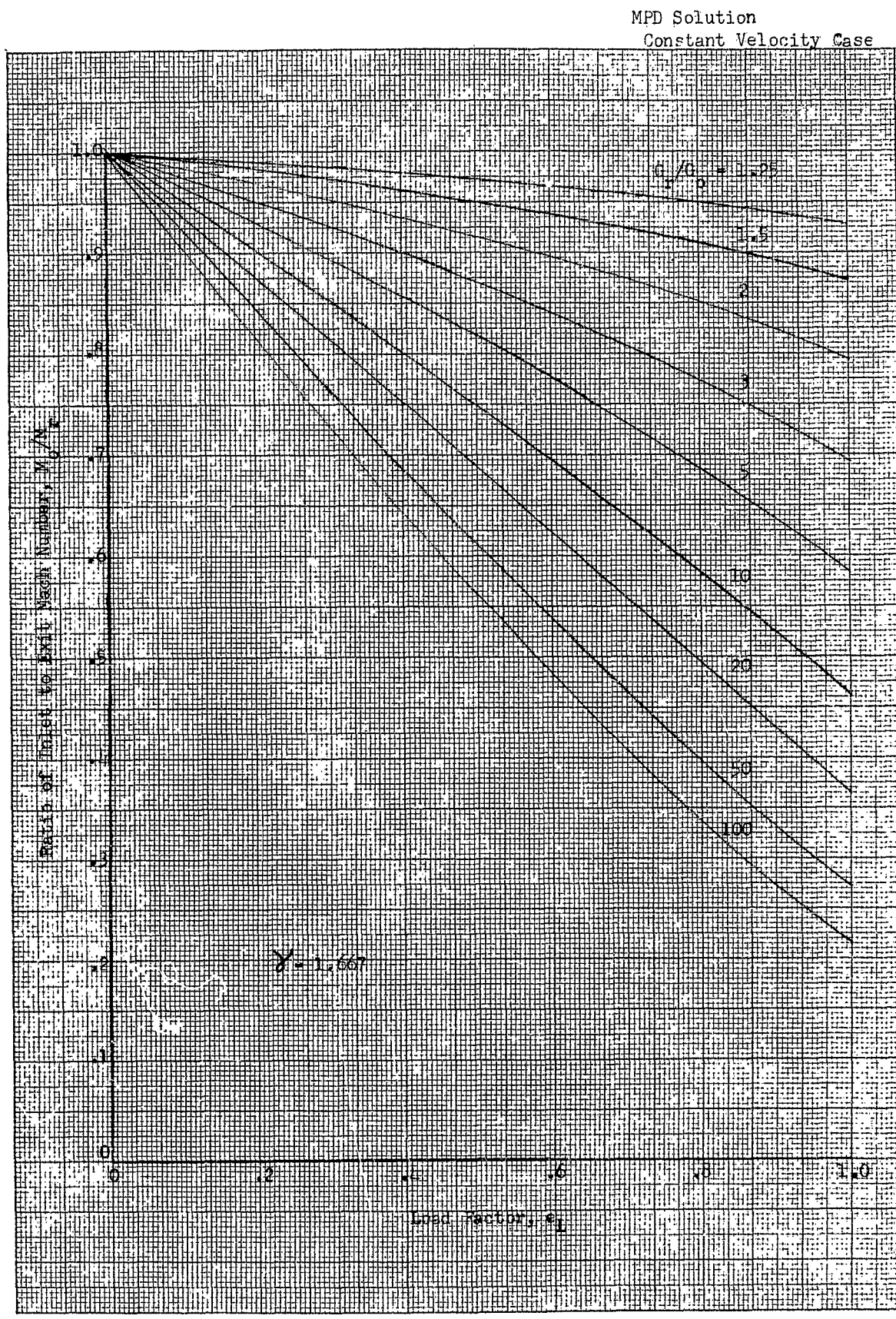

Ratio of Mach Number versus Load Factor

MPD Solution
Constant Velocity Case

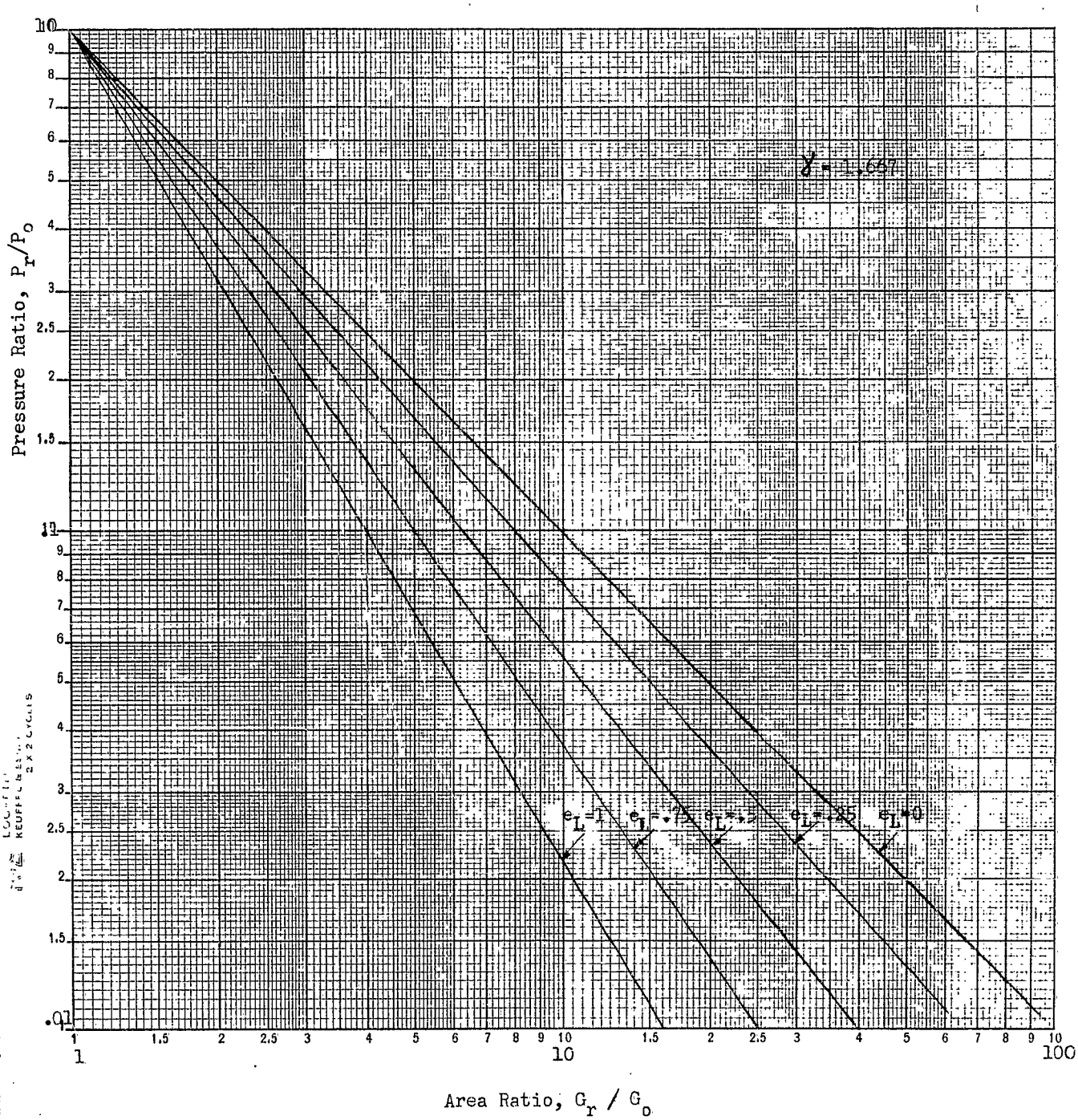

Pressure Ratio versus Area Ratio

MPD Solution
Constant Velocity Case

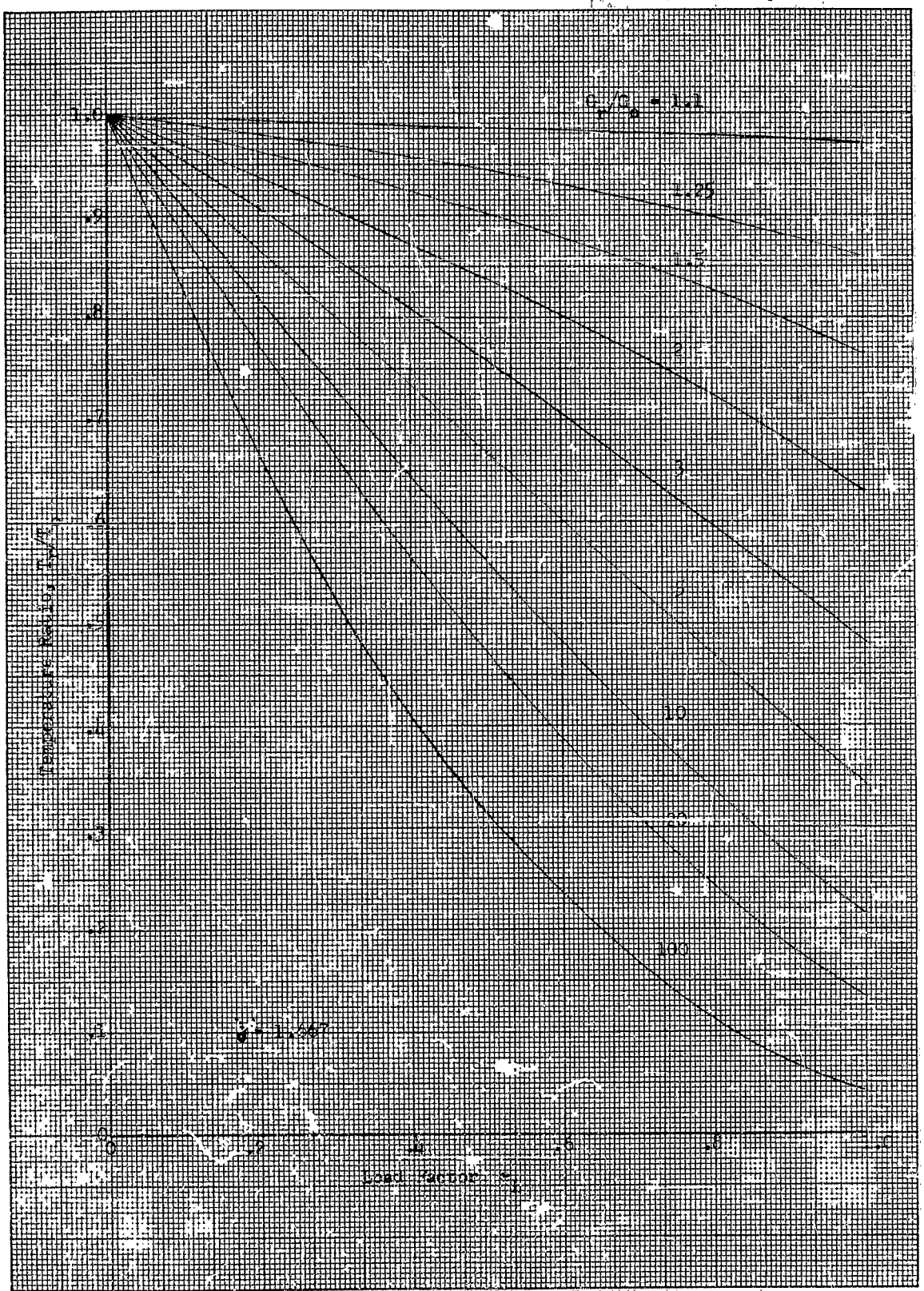

Temperature Ratio versus Load Factor

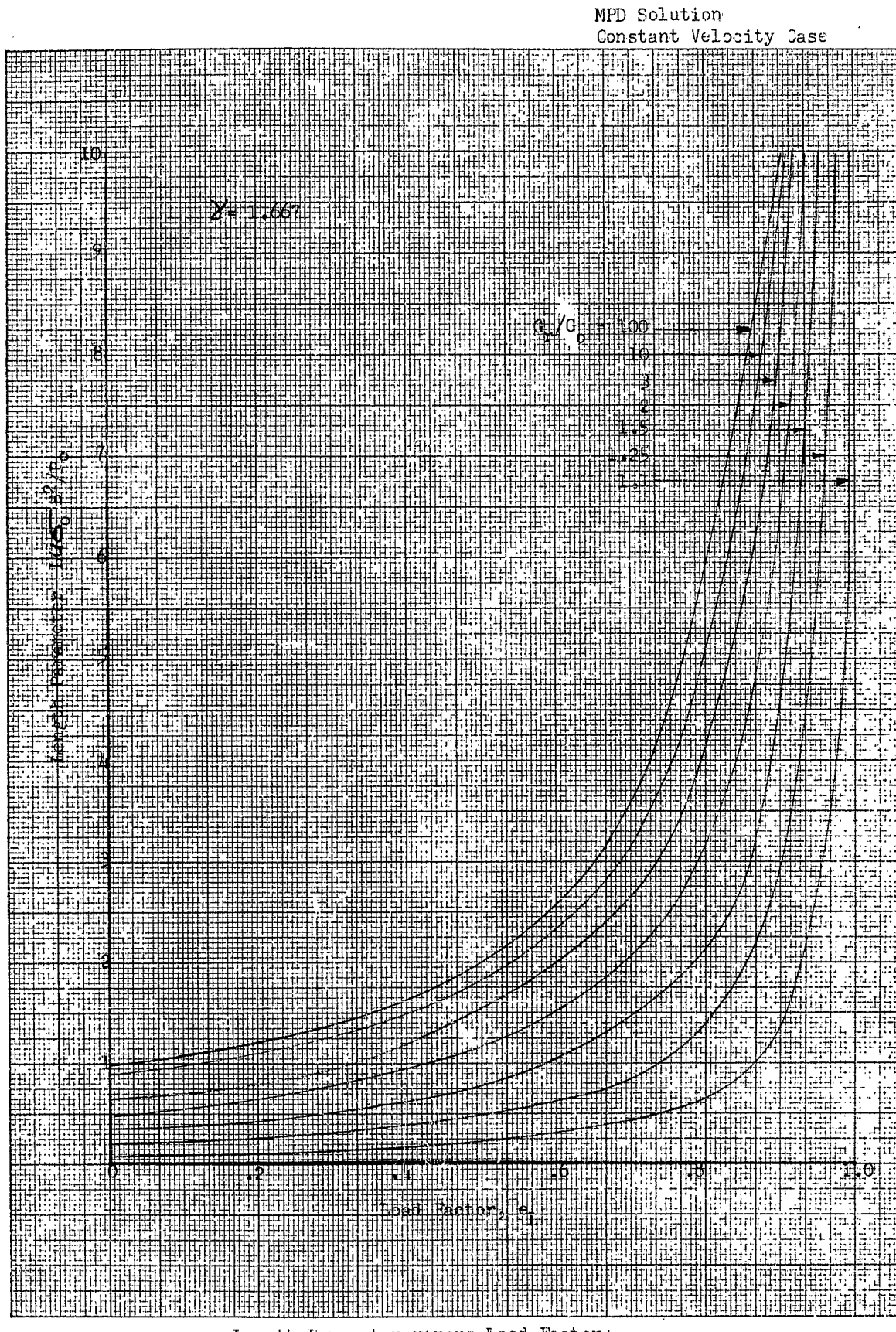

Length Parameter versus Load Factor

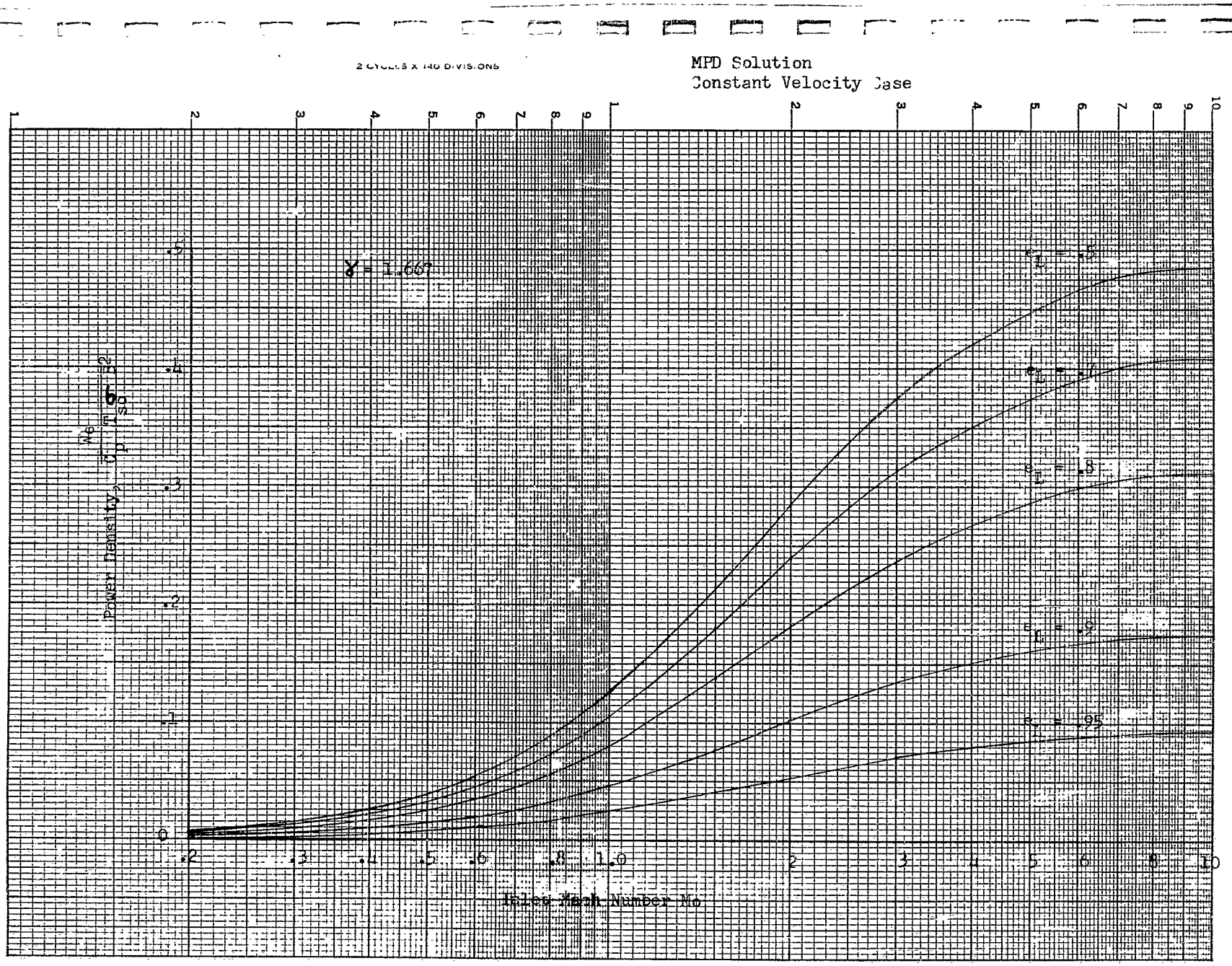

Power Density vs Inlet Mach Number

MPD Solution
Constant Velocity Case

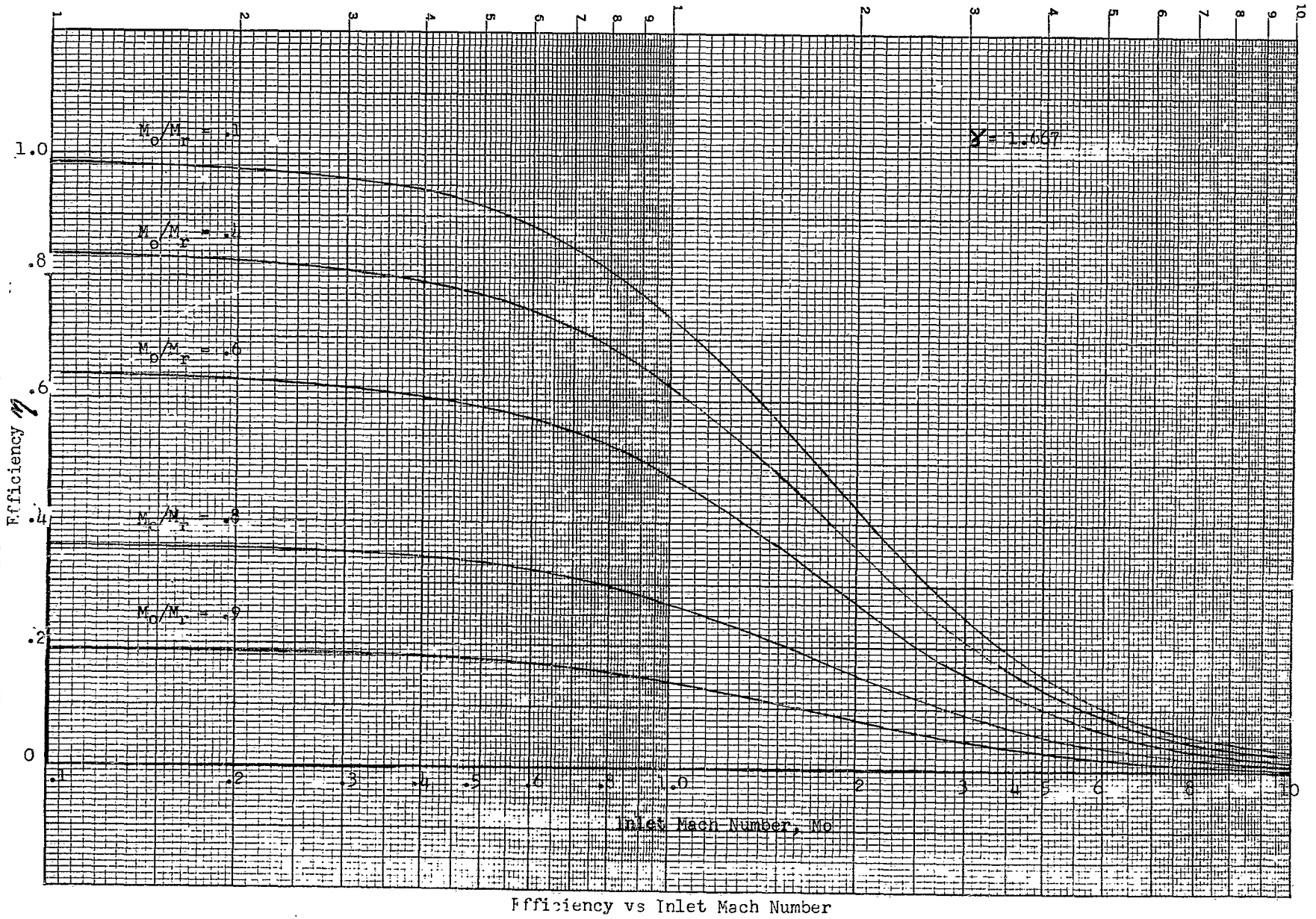

Efficiency vs Inlet Mach Number

where p_r and M_r are the pressure and Mach number at the end of the magnetic field - current interaction region and L is the length of the duct corresponding to exit Mach number, M_r, and is given by

$$L = \frac{p_o}{u\sigma_o B^2(1 - e_L)}\left[1 - \left(\frac{M_o}{M_r}\right)^{2/\alpha}\right] = \frac{p_o}{u\sigma_o B^2(1 - e_L)}\left[1 - \frac{p_r}{p_o}\right] \qquad (45)$$

In the following figures the solution equations presented above for the constant velocity segmented electrodes Faraday generator case are presented in universal dimensionless form. Thus, for example, if we fix the electric load condition (viz., e_L) and the exit to inlet area ratio (viz., G_r/G_o) we determine the ratio of inlet to exit Mach number (vix., M_o/M_r), the ratio of exit to inlet pressure (viz., p_r/p_o), the ratio of exit to inlet temperature (viz., T_r/T_o) and the generator length parameter (viz., $Lu\sigma_o B^2/p_o$). Next by choosing the inlet Mach number, M_o, temperature, T_o, and pressure p_o we can now calculate the generator length, L, generator efficiency, η, and the generator average power density, w_e, (in terms of the power density factor $C_p T_{So}\sigma_o B^2$) where $T_{So} = T_o\left(1 + \frac{\gamma - 1}{2} M_o^2\right)$.

B. Constant Area Duct Segmented Electrodes Faraday Generator with Constant Electrical Conductivity, σ_o, and Constant Internal Voltage Drop Between Each Pair of Electrodes Along the Length of the Duct

In this case the current density in the x direction, J_x is zero and, hence, the electric field in the flow direction is given by equation (24), viz.,

$$\mathcal{E}_x = \beta(\mathcal{E}_y - uB) \qquad (24)$$

And the current density in the y direction is again given by equation (25), viz.,

$$J_y = \sigma_o(\mathcal{E}_y - uB) \qquad (25)$$

If the condition is further observed that in the case of non-equilibrium ionization conductivity resulting from electron heating* it is necessary to maintain the internal electric field, $\mathcal{E}_e$, and hence also the current density, J_y, constants along the duct length, then Ohm's law (or equation 25) becomes

$$J_y = -\sigma_o (uB - \mathcal{E}_y) = -\sigma_o \mathcal{E}_e = -\sigma_o u_o B(1 - e_L) = \text{constant} \qquad (46)$$

For the constant area duct and under the condition of Ohm's law in equation (46) the continuity equation, the equation of motion, the energy equations and the equation of state now take on the following forms, respectively:

a. Continuity Equation

$$\rho u = \rho_o u_o = \text{constant} \qquad (47)$$

b. Equation of Motion

$$\rho_o u_o \frac{du}{dx} + \frac{dp}{dx} = J_y B = -u_o \sigma_o B^2 (1 - e_L) = \text{constant} \qquad (48)$$

c. Energy Equation

$$\rho_o u_o \frac{d}{dx}\left[\frac{1}{(\gamma - 1)M^2} + \frac{1}{2}\right] u^2 = \left(uB + \frac{1}{\sigma_o} J_y\right) J_y = \mathcal{E}_y J_y$$

$$= -\left[uB - u_o B(1 - e_L)\right] \sigma_o u_o B(1 - e_L)$$

$$= -\left[u - u_o(1 - e_L)\right] u_o \sigma_o B^2 (1 - e_L) \qquad (49)$$

d. Equation of State

$$p = \rho RT = \rho \frac{u^2}{\gamma M^2} = \rho_o u_o \frac{u}{\gamma M^2} \quad (\text{since } u^2 = M^2 \gamma RT) \qquad (50)$$

---

* See paper by M. E. Talaat "Magnetoplasmadynamic Electrical Power Generation with Non-Equilibrium Ionization," presented September 6, 1962 at the Symposium on Magnetoplasmadynamic Electrical Power Generation at Kings College, Newcastle Upon Tyne, England. Paper under publication in Advanced Energy Conversion Journal, 1963; see also Martin Semi-annual Report MND-2939.

By substituting the expression for the pressure, p, from equation (50) into equation (48) we get

$$\rho_o u_o \frac{d}{dx}\left[\left(1 + \frac{1}{\gamma M^2}\right)u\right] = - u_o \sigma_o B^2 (1 - e_L) \tag{51}$$

Now by multiplying equation (51) by $\left[u - u_o(1 - e_L)\right]$ and equating the lefthand side of the result with the left hand side of equation (49) we get equation (52) which gives the differential relation between the velocity, u, and the Mach number, M, viz.,

$$\left[u - u_o(1 - e_L)\right]\frac{d}{dx}\left[\left(1 + \frac{1}{\gamma M^2}\right)u\right] = \frac{d}{dx}\left[\left\{\frac{1}{(\gamma - 1)M^2} + \frac{1}{2}\right\} u^2\right] \tag{52}$$

Now, let $u_o(1 - e_L) = u_e$ and substitute $\frac{\gamma RT}{u^2}$ for $\frac{1}{M^2}$ in equation(52), hence

$$(u - u_e)d\left(u + \frac{RT}{u}\right) = d\left[\frac{\gamma}{\gamma - 1}RT + \frac{1}{2}u^2\right] = d\left(C_p T + \frac{1}{2}u^2\right) = C_p dT + udu \tag{53}$$

or

$$(u - u_e)\left[du + \frac{R}{u}dT - \frac{RT}{u^2}du\right] = C_p dT + udu \tag{54}$$

and since $C_p = C_V + R$, rearranging terms in equation (54) we get

$$\left[RT(u - u_e) + u^2 u_e\right]du + \left[u^2 C_V + uu_e R\right]dT = 0 \tag{55}$$

Now let $T = vu$ hence, (56)

$$dT = vdu + udv \tag{57}$$

Substituting from equations (56) and (57) into equation (55) and eliminating T and dT from equation (55) we get after rearranging the terms

$$(C_p v + u_e)du = - (uC_V + u_e R)dv \tag{58}$$

or

$$\frac{1}{C_p}\frac{C_p dv}{C_p v + u_e} = - \frac{1}{C_V}\frac{C_V du}{C_V u + Ru_e} \tag{59}$$

The relation between the velocity, u, and the temperature, T, or Mach number, M, can be readily obtained by integrating equation (59) subject to the boundary conditions that at x = 0, v = v_o, u = u_o, T = T_o and M = M_o. Thus,

$$\frac{C_p v + u_e}{C_p v_o + u_e} = \left[\frac{C_V u_o + R u_e}{C_V u + R u_e}\right]^{\gamma} \tag{60}$$

and since $v = \frac{T}{u}$, $C_p T = \frac{\gamma}{\gamma - 1} RT = \frac{u^2}{(\gamma - 1)M^2}$, hence, $C_p v = C_p \frac{T}{u} = \frac{u}{(\gamma - 1)M^2}$

and

$$\frac{u}{(\gamma - 1)M^2} + u_e = \left[\frac{u_o}{(\gamma - 1) M_o^2} + u_e\right]\left[\frac{C_V u_o + R u_e}{C_V u + R u_e}\right]^{\gamma} \tag{61}$$

let the velocity ratio $s = \frac{u}{u_o}$, and since $\frac{R}{C_V} = (\gamma - 1)$ and recalling that $u_e = (1 - e_L)u_o$ we get by substitution into equation (61) the following relation between the velocity ratio and the Mach numbers

$$\left[\frac{s}{M^2} + (\gamma - 1)(1 - e_L)\right] = \left[\frac{1}{M_o^2} + (\gamma - 1)(1 - e_L)\right]\left[\frac{1 + (\gamma - 1)(1 - e_L)}{s + (\gamma - 1)(1 - e_L)}\right]^{\gamma} \tag{62}$$

Note that at $e_L = 1$, $\frac{s}{M^2} = \frac{1}{M_o^2}\frac{1}{s^{\gamma}}$ or $s = \left(\frac{M}{M_o}\right)^{2/(\gamma + 1)}$ which checks the isentropic flow relation as it should.

Next, solution of the equation of motion (equation 51) gives the relation between the axial distance, x, measured from the inlet to the magnetic field-current interaction region and the corresponding velocity ratio, s, and Mach number, M, for a given inlet Mach number and a given electric load factor, e_L, thus by integrating equation (63)

$$\frac{d}{dx}\left[s + \frac{s}{\gamma M^2}\right] = -\frac{\sigma_o B^2}{\rho_o u_o}(1 - e_L) \tag{63}$$

subject to the boundary conditions that at $x = 0$ $s = 1$ and $M = M_o$ we get

$$\left(1 + \frac{1}{\gamma M_o^2}\right) - s\left(1 + \frac{1}{\gamma M^2}\right) = \frac{\sigma_o B^2}{\rho_o u_o}(1 - e_L)\, x \tag{64}$$

If the Mach number at the exit is M_r and the corresponding velocity ratio is s_r the generator active length, L, can be obtained from equation (64), thus

$$\frac{L\sigma_o B^2}{\rho_o u_o} = \frac{1}{(1 - e_L)}\left[\left(1 + \frac{1}{\gamma M_o^2}\right) - s_r\left(1 + \frac{1}{\gamma M_r^2}\right)\right] \tag{65}$$

In equation (65) once M_r is chosen the corresponding s_r can be obtained from equation (62) which gives the relation between M and s for a given inlet Mach number, M_o, and a given electric load factor, e_L. Equation (65) can thus be used to determine L for a given set of operating conditions (M_o, e_L, T_o, M_r and s_r) or determine the exit Mach number and velocity ratio once L is chosen.

The output power is given by the following expression

$$W_e = \int_o^L DGJ_y \mathcal{E}_y dx \tag{66}$$

Substituting for $J_y \mathcal{E}_y dx$ from equation (49) into equation (66) the expression for the output power reduces to the following

$$W_e = DG\rho_o u_o \int_{u_o, M_o}^{u, M} d\left[\frac{u^2}{(\gamma - 1)M^2} + \frac{u^2}{2}\right]$$

$$= DG\rho_o u_o u_o^2 \int_{1, M_o}^{s, M} d\left[\frac{s^2}{(\gamma - 1)M^2} + \frac{s^2}{2}\right]$$

$$= DG\rho_o u_o u_o^2 \left[\frac{1}{(\gamma - 1)}\left(\frac{s^2}{M^2} - \frac{1}{M_o^2}\right) + \frac{1}{2}(s^2 - 1)\right] \tag{67}$$

The expression for average output power density, w_e, is next obtained by dividing the expression for output power, equation (67), by the volume DGL and using the expression for L as given by equation (65). Thus,

$$w_e = \frac{W_e}{DGL} = u_o^2 \sigma_o B^2 \ (1 - e_L) \frac{\left[\frac{1}{(\gamma - 1)}\left(\frac{s_r^2}{M_r^2} - \frac{1}{M_o^2}\right) + \frac{1}{2}(s_r^2 - 1)\right]}{\left[\left(\frac{1}{\gamma M_o^2} + 1\right) - \left(\frac{1}{\gamma M_r^2} + 1\right) s_r\right]} \tag{68}$$

Now since

$$u_o^2 = \gamma R T_o M_o^2 = \gamma \frac{R_o}{Z} T_o M_o^2 = \gamma \frac{R_o}{Z} \frac{T_{so}}{1 + \frac{\gamma - 1}{2} M_o^2} M_o^2 \tag{69}$$

the expression for the average output power density can be written as follows

$$\frac{w_e}{\frac{\gamma}{(\gamma - 1)} \frac{R_o}{Z} T_{so} \sigma_o B^2} = \frac{w_e}{C_p T_{so} \sigma_o B^2} = (1 - e_L) \frac{\gamma}{\frac{\gamma - 1}{2} + \frac{1}{M_o^2}} \frac{s_r^2 \left[\frac{\gamma - 1}{2} + \frac{1}{M_r^2}\right] - \left[\frac{\gamma - 1}{2} + \frac{1}{M_o^2}\right]}{\left[\left(\gamma + \frac{1}{M_o^2}\right) - s_r\left(\gamma + \frac{1}{M_r^2}\right)\right]} \tag{70}$$

Thus for a given gas at a given stagnation temperature, T_{so}, inlet and exit Mach numbers, M_o and M_r, electric load factor, e_L, and exit to inlet velocity, s_r, (see equation (62) for dependence of s_r on M_r, M_o and e_L) we can evaluate the average power density, w_e.

Finally the expression for power extraction efficiency is given by the ratio of output power to total enthalpy at the duct inlet (see case A and Ref. 1)

$$\eta = \frac{-W_e}{W_o} = 1 - \frac{\frac{1}{(\gamma - 1) M_r^2} + \frac{1}{2}}{\frac{1}{(\gamma - 1) M_o^2} + \frac{1}{2}} s_r^2 \tag{71}$$

where again the exit to inlet velocity ratio, s_r, is determined from equation (62) once M_r, M_o and e_L are specified.

In the following figures the solution equations presented above for the constant area duct segmented electrode Faraday generator case are presented in universal dimensionless forms. The exit to inlet velocity ratio is thus plotted versus the inlet Mach number, M_o, for a constant exit Mach number $M_r = 1$ (the choke condition since in this case the flow is choke limited) and electric load factor e_L of 0.5, 0.7 and 0.9. Similar figures are given for the exit to inlet temperature ratio, $(T_r/T_o) = s_r^2(M_o^2/M_r^2)$ and the exit to inlet pressure ratio, $(p_r/p_o) = s_r(M_o^2/M_r^2)$ again for $M_r = 1$ and $e_L = 0.5$, 0.7 and 0.9.

The length parameter $(L\sigma_o B^2/\rho_o u_o)$ is plotted versus the inlet Mach number, M_o, for an exit Mach number, $M_r = 1$, and load factors $e_L = 0.5$, 0.7 and 0.9. Similarly, the energy conversion efficiency, η, is plotted versus the inlet Mach number, M_o, for an exit Mach number, $M_p = 1$, and load factors $e_L = 0.5$, 0.7 and 0.9. The power density parameter $(w_e/C_p T_{so}\sigma_o B^2)$ is also plotted versus the inlet Mach number, M_o, for an exit Mach number, $M_r = 1$ and load factors $e_L = 0.5$, 0.7, 0.8, 0.85 and 0.9. Note that maximum (100%) efficiency for any load factor, e_L, is approached as the inlet Mach number, M_o, approaches zero, while zero efficiency is approached as M_o approaches Mach one. When the inlet Mach number, M_o, approaches ∞ the efficiency, η_∞, for any load factor, e_L, approaches the value given by

$$\eta_\infty = 1 - 4 s_\infty^2 \tag{72}$$

where s_∞ is the exit to inlet velocity ratio for $M_o \to \infty$ and is given by

$$s_\infty = \left\{(\gamma - 1)(1 - e_L)\right\}^{0.375} \left\{1 + (\gamma - 1)(1 - e_L)\right\}^{0.625} - (\gamma - 1)(1 - e_L) \tag{73}$$

Thus for a monatomic gas at load factors e_L = 0.5, 0.7, 0.8, 0.85 and 0.9 the exit to inlet velocity ratios s_∞ are 0.4585, 0.413, 0.3733, 0.348 and 0.3113, respectively and the efficiencies, η_∞ , approached as M_o approaches ∞ are 0.160, 0.318, 0.444, 0.5185 and 0.613, respectively.

The power density parameter $(w_e/C_p T_{so} \sigma_o B^2)$, on the other hand, approaches zero as the inlet Mach number approaches zero. As the inlet Mach number approaches one the power density parameter $(w_e/C_p T_{so} \sigma_o B^2)$ approaches the following expression

$$\left.\frac{w_e}{C_p T_{so} \sigma_o B^2}\right]_{M_o \to 1} = (1 - e_L) \frac{\gamma}{1 + \frac{\gamma - 1}{2}} \left[1 - \frac{1}{\gamma}\left\{1 + (\gamma - 1)(1 - e_L)\right\}\right] \qquad (74)$$

Thus for a monatomic gas at load factors e_L = 0.5, 0.7, 0.8, 0.85 and 0.9 the power density factors approached as M_o approaches unity are 0.125, 0.105, 0.08, 0.06375 and 0.045, respectively. As the inlet Mach number approaches infinity the power density factor approaches the limit

$$\left.\frac{w_e}{C_p T_{so} \sigma_o B^2}\right]_{M_o \to \infty} = (1 - e_L) \frac{\gamma}{(\gamma - 1)} \frac{(\gamma - 1) - (\gamma + 1)s_\infty^2}{\gamma - (\gamma + 1)s_\infty} \qquad (75)$$

Thus for a monatomic gas at load factors e_L = 0.5, 0.7, 0.8, 0.85 and 0.9 the power density factors approached as M_o approaches infinity are 0.300, 0.281, 0.221, 0.175 and 0.122, respectively.

Velocity Ratio vs Inlet Mach Number

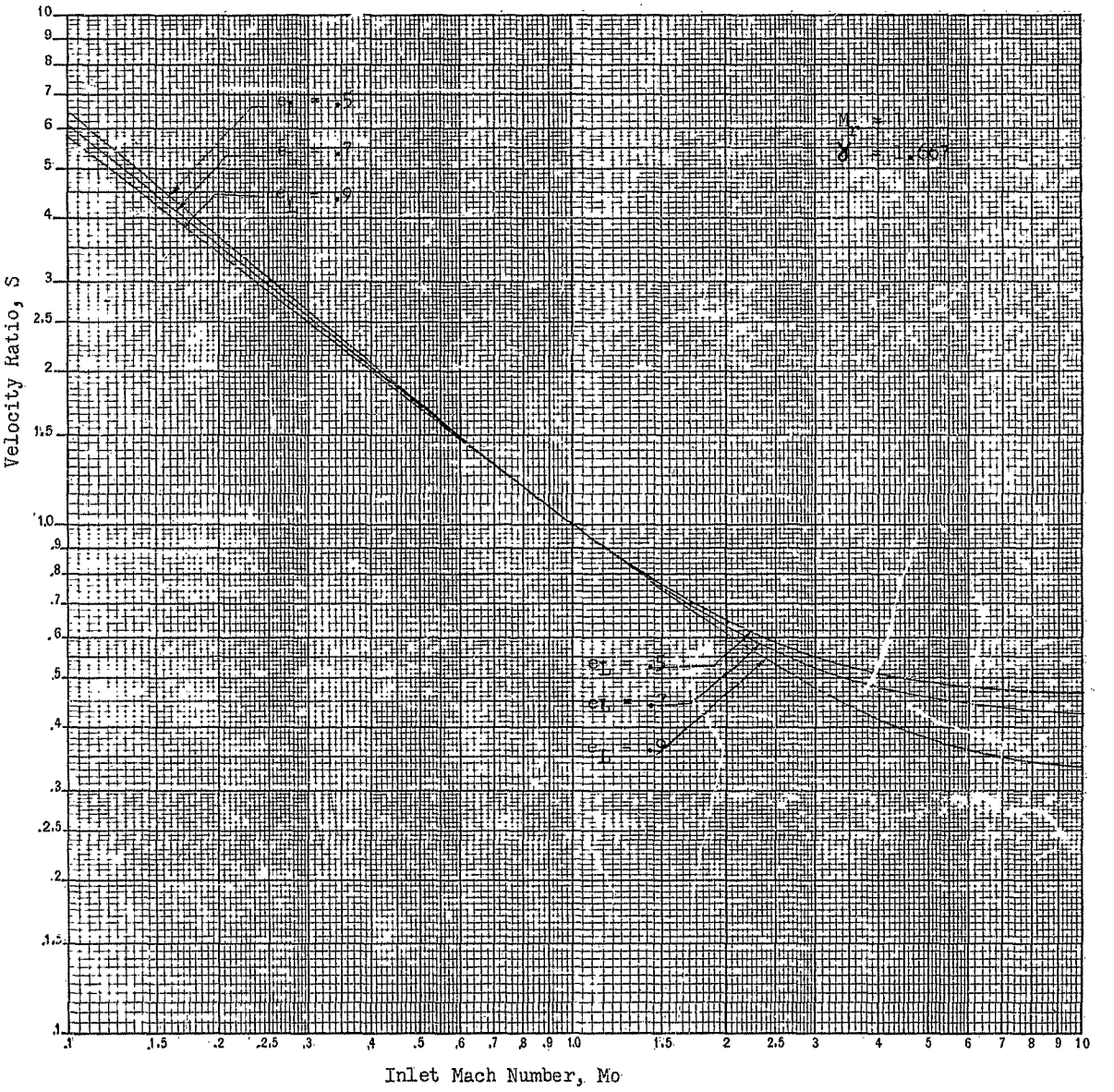

MPD Solution
Constant Current Case

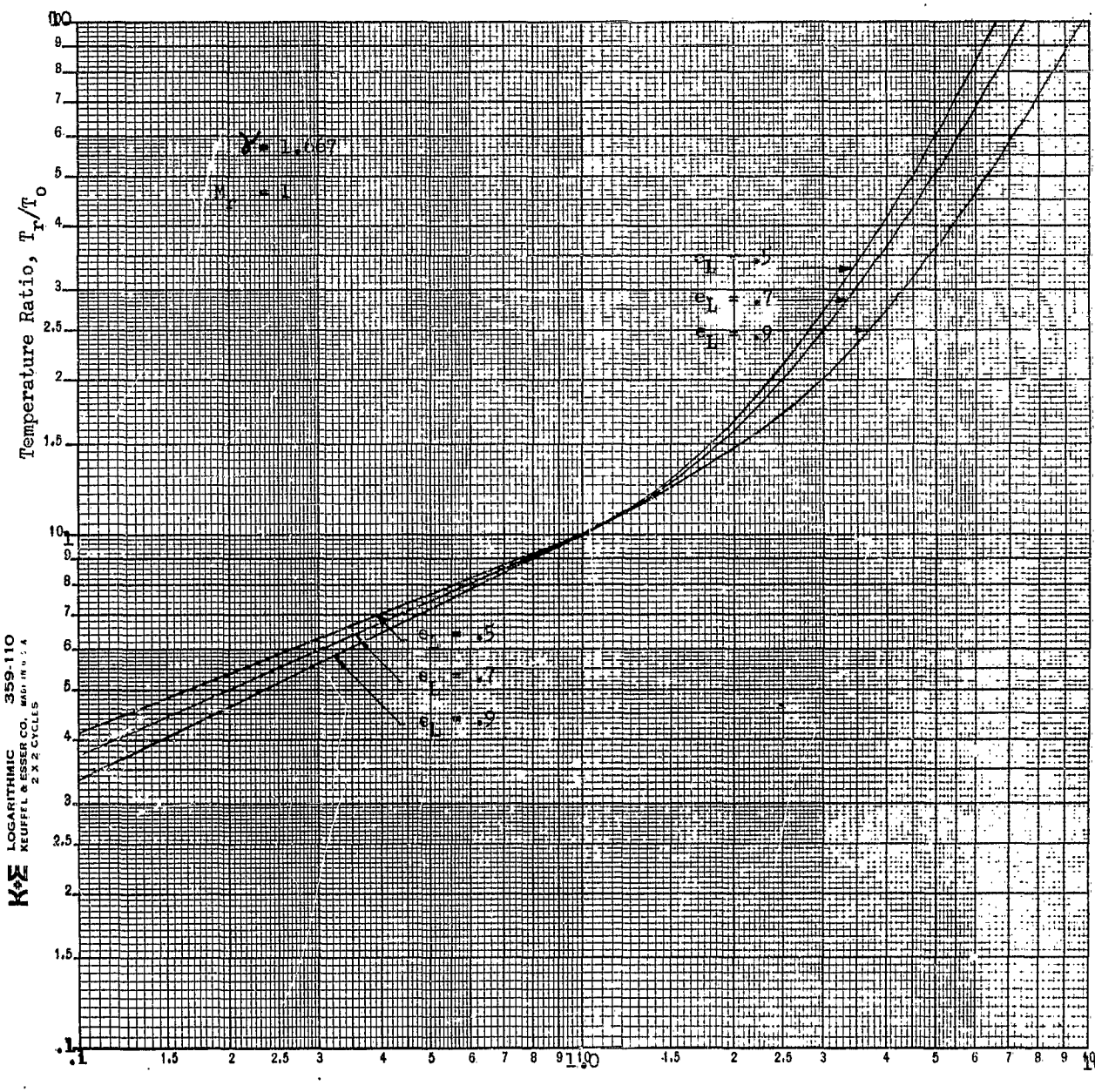

Temperature Ratio versus Inlet Mach Number

MPD Solution
Constant Current Case

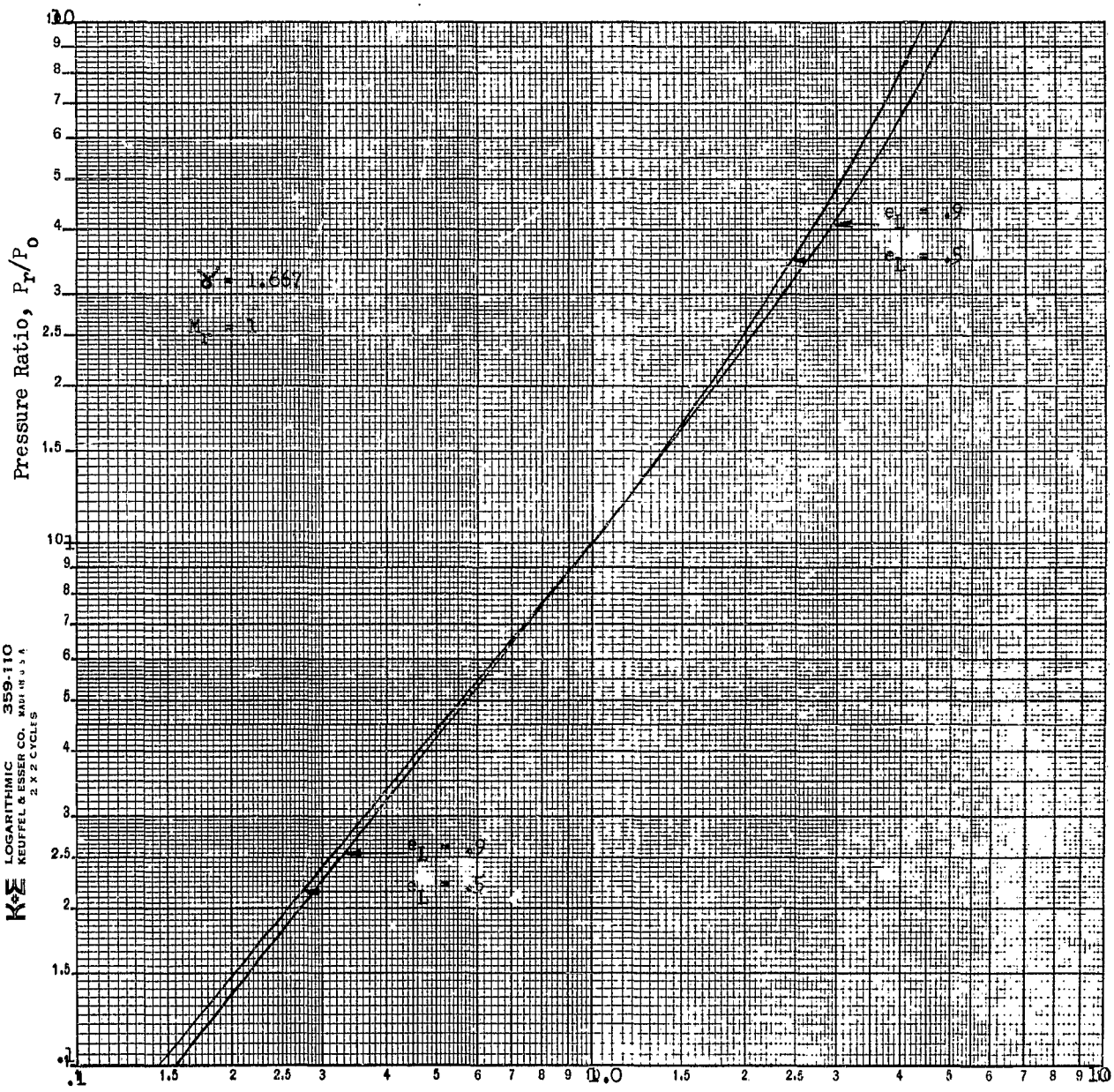

Pressure Ratio versus Inlet Mach Number

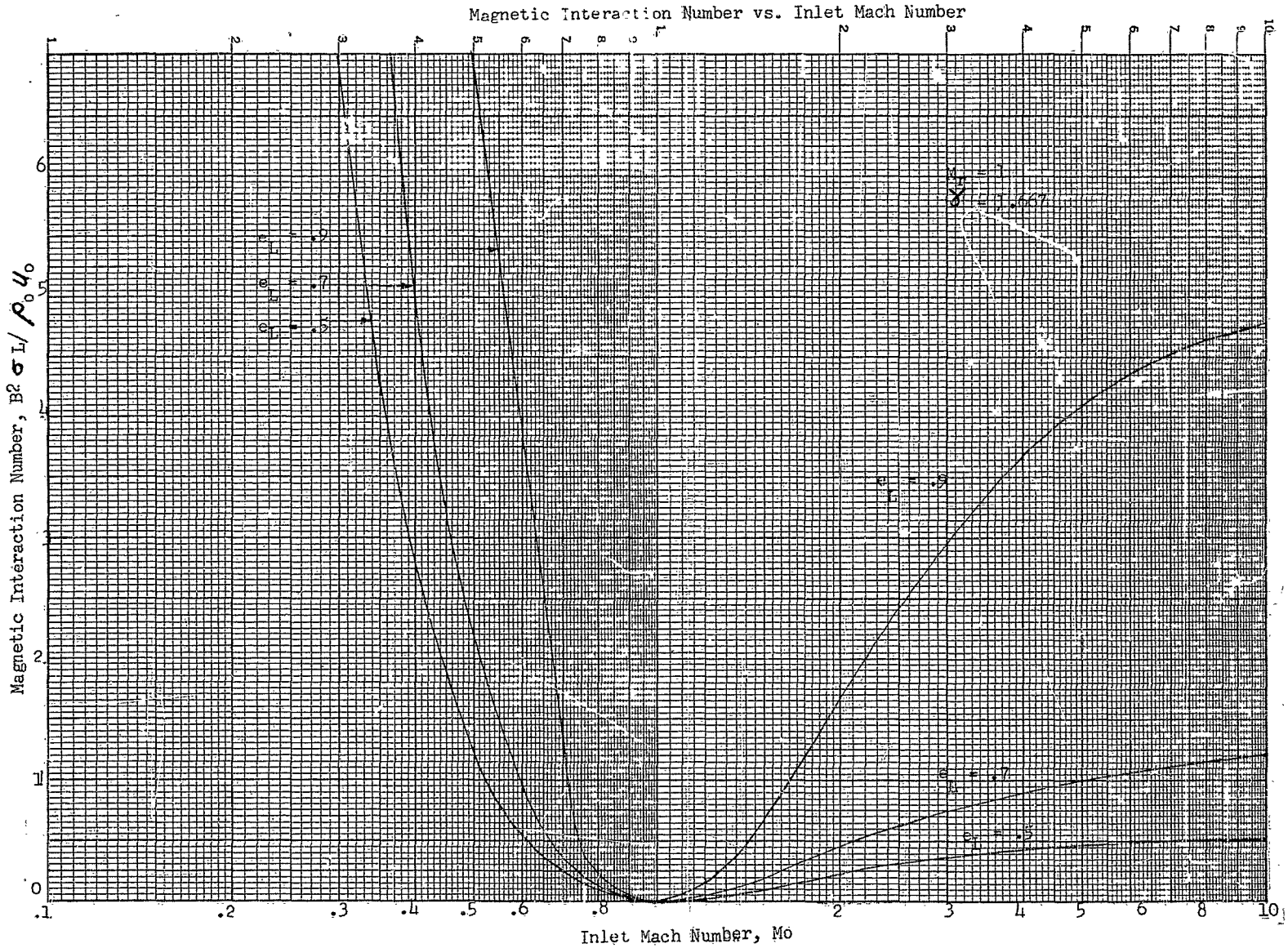
Magnetic Interaction Number vs. Inlet Mach Number
Magnetic Interaction Number, $B^2 \sigma L / \rho_o u_o$
Inlet Mach Number, Mo
$\sigma_L = .9$
$\sigma_L = .7$
$\sigma_L = .5$
$M_{cr} = 3.607$
$\sigma_L = .9$
$\sigma_L = .7$
$\sigma_L = .5$
0
1
2
6
.1
.2
.3
.4
.5
.6
.8
2
3
4
5
6
8
10

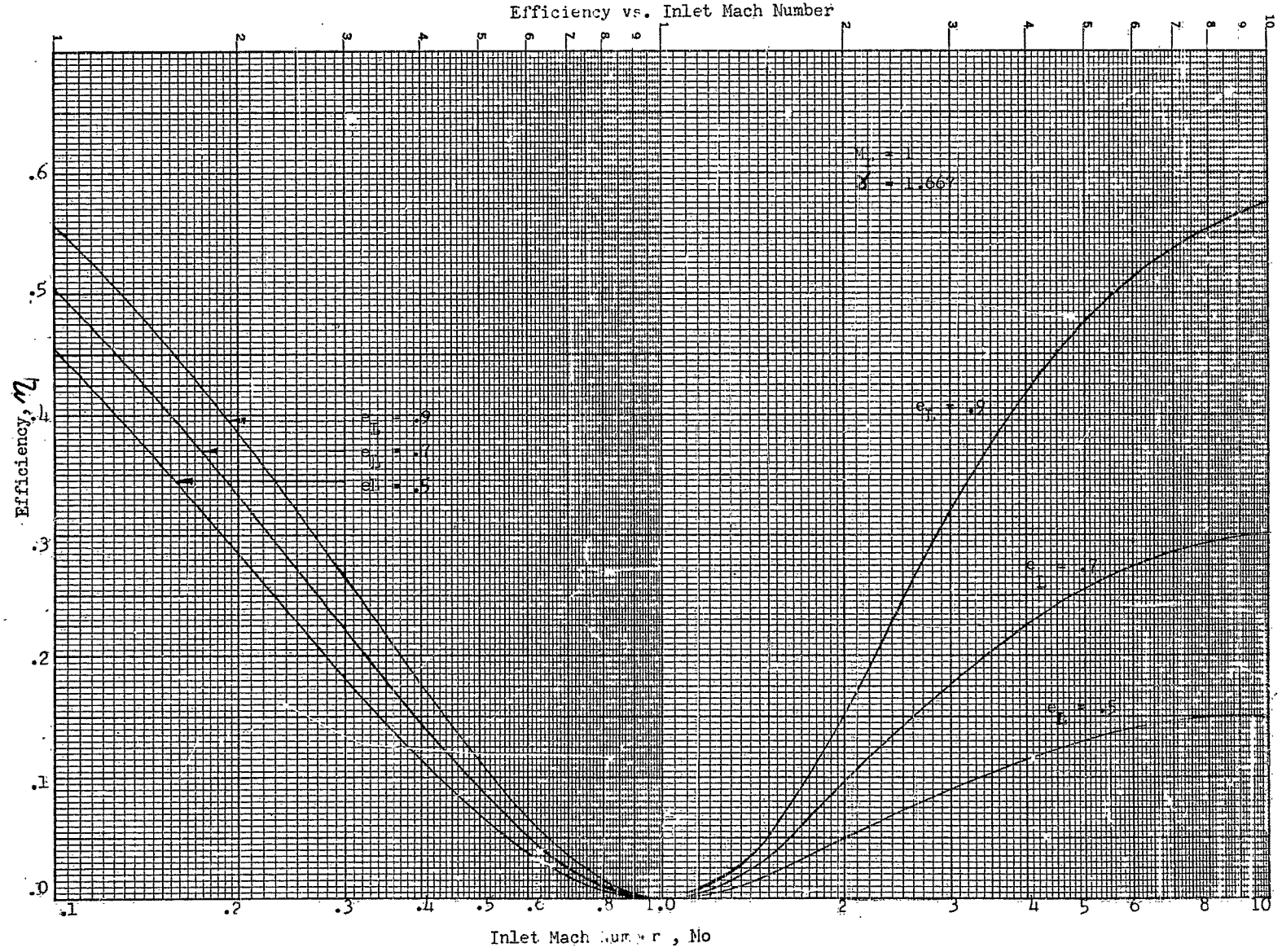
Efficiency vs. Inlet Mach Number
Efficiency, η
Inlet Mach Number , No
M₁ = 1
γ = 1.667
e_d = .9
e_d = .7
e_d = .5
e_d = .9
e_d = .7
e_d = .5
.0
.1
.2
.3
.4
.5
.6
1.0
2
3
4
5
6
7
8
9
10

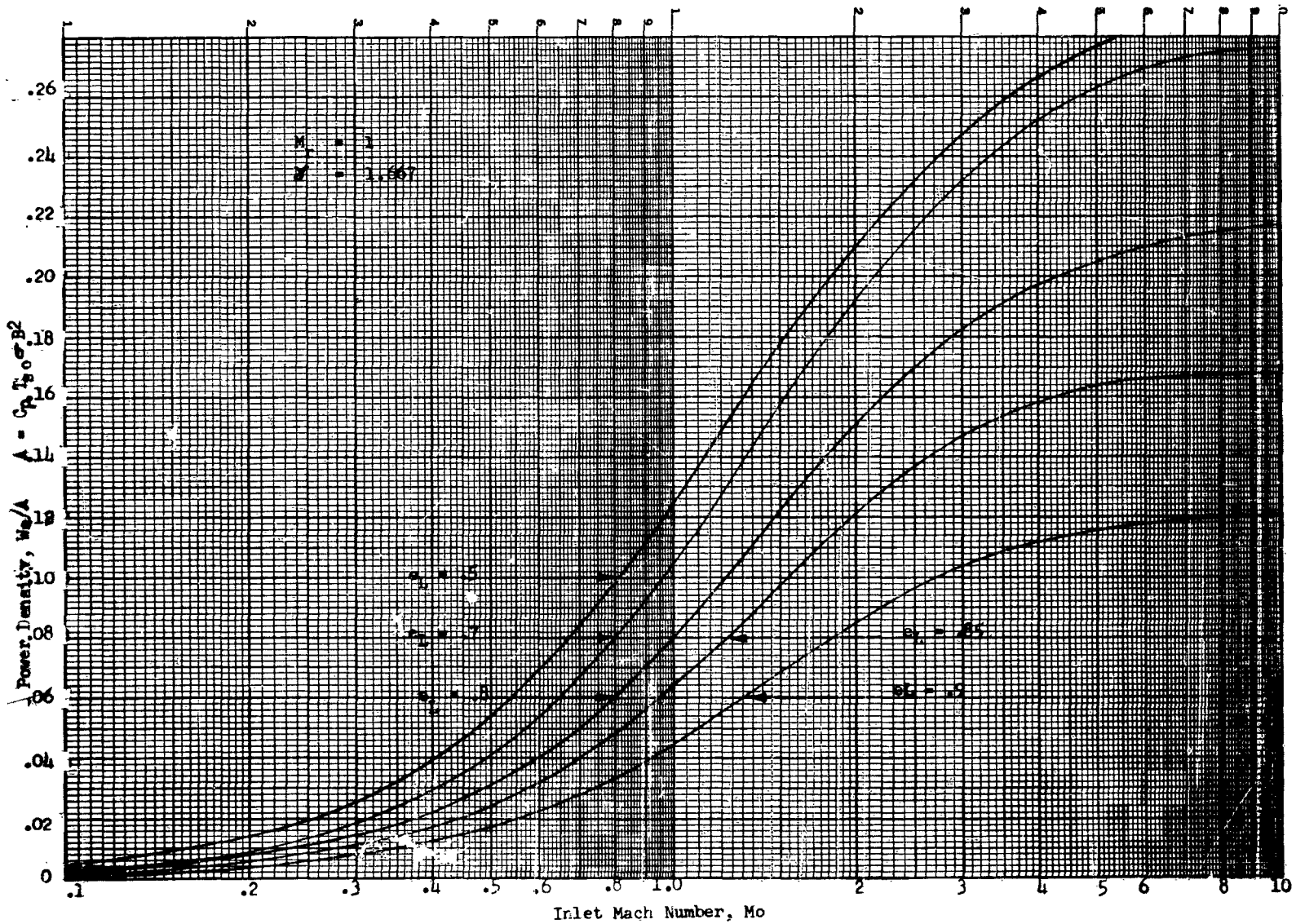
M_1 = 1
γ = 1.667
σ_1 = .95
σ_1 = .9
σ_1 = .8
σ_1 = .85
σ_1 = .5
Power Density, We/A $A = C_R T_{so} \sigma B^2$
Inlet Mach Number, Mo
.26
.24
.22
.20
.18
.16
.14
.12
.10
.08
.06
.04
.02
0
.1
.2
.3
.4
.5
.6
.8
1.0
2
3
4
5
6
8
10

C. Constant Area Duct Segmented Electrodes Faraday Generator with Constant Electrical Conductivity, σ_o, and Constant Electrical Load Resistance for Each Electrode Pair Along the Duct

In this case the current density in the x-direction is zero and the current density in the y-direction is again given by

$$J_y = \sigma_o(\mathcal{E}_y - uB) = -\sigma_o uB\left(1 - \frac{\mathcal{E}_y}{uB}\right) \tag{76}$$

Now if we let $(\mathcal{E}_y/uB) = e_L = \text{constant}$ (77)

for each pair of opposite electrodes, then the expression for the current J_y can be written as follows

$$J_y = -\sigma_o \frac{\mathcal{E}_y}{e_L}(1 - e_L) \tag{78}$$

which when solved for $(\mathcal{E}_y/J_y)$ yields the following expression

$$(\mathcal{E}_y/J_y) = -e_L/\sigma_o(1 - e_L) \tag{79}$$

Equation (79) in essence states that the load condition expressed by equation (77) exists when the load resistance is maintained constant for each pair of electrodes along the generator duct.

The equations governing the behavior of the MPD generator, under these conditions, then take the following forms

1) Ohm's Law

$$J_y = -\sigma_o uB(1 - e_L) \tag{80}$$

2) Continuity

$$\rho u = \rho_o u_o = \text{constant} \tag{81}$$

3) Equation of Motion

$$\rho_o u_o \frac{du}{dx} + \frac{dp}{dx} = J_y B = -u\sigma_o B^2(1 - e_L) \tag{82}$$

4) Energy Equation

$$-\rho_o u_o \frac{d}{dx}\left[\frac{u^2}{(\gamma-1)M^2} + \frac{u^2}{2}\right] = u^2 \sigma_o B^2 e_L(1 - e_L) \tag{83}$$

5) Equation of State

$$p = \rho RT = \rho \frac{u^2}{\gamma M^2} = \rho_o u_o \frac{u}{\gamma M^2} \tag{84}$$

Solution of these equations yields the following expression for the velocity ratio, s, in terms of the load factor, e_L, the inlet Mach number, M_o, and the Mach number, M, at any point at distance x from the inlet to the magnetic field - current interaction region

$$s = \left(\frac{u}{u_o}\right) = \left[\frac{M^2(aM_o^2 + b)}{M_o^2(aM^2 + b)}\right]^{(c/b)} \tag{85}$$

where

$$a = \gamma(\gamma - 1)(1 - e_L) \tag{86}$$

$$b = 2\gamma - (\gamma - 1)e_L \tag{87}$$

$$c = \gamma - (\gamma - 1)e_L \tag{88}$$

Solution for the relation between the distance x, the load factor, e_L, the inlet Mach number, M_o, the Mach number, M, at the distance yields

$$x \frac{\sigma_o B^2}{\rho_o u_o} = \frac{1}{b(1 - e_L)}\left(\frac{1}{M_o^2} - \frac{1}{M^2}\right) - \frac{c(\gamma + 1)}{b^2(1 - e_L)} \ln \frac{M^2(aM_o^2 + b)}{M_o^2(aM^2 + b)} \tag{89}$$

The expressions for the output power and efficiency η are given in the following and are derived by following similar arguments as those used in deriving parallel expressions for cases A and B.

Thus

$$W_e = -GD \int_0^L J_y \mathcal{E}_y \, dx = - GD \rho_o u_o u_o^2 \int_{1,M_o}^{s,M} d\left[\left\{ \frac{1}{(\gamma-1)M^2} + \frac{1}{2} \right\} s^2 \right]$$

$$= (GD \rho_o u_o) \, u_o^2 \left[\left\{ \frac{1}{(\gamma-1)M_o^2} + \frac{1}{2} \right\} - \left\{ \frac{1}{(\gamma-1)M^2} + \frac{1}{2} \right\} s^2 \right]$$

$$= (GD \rho_o u_o) M_o^2 \gamma R T_o \frac{1}{(\gamma-1)} \left[\frac{1}{M_o^2} + \frac{\gamma-1}{2} \right] \left[1 - \frac{\frac{1}{(\gamma-1)M^2} + \frac{1}{2}}{\frac{1}{(\gamma-1)M_o^2} + \frac{1}{2}} s^2 \right]$$

$$= (GD \rho_o u_o) \frac{\gamma}{\gamma-1} R T_o \left[1 + \frac{\gamma-1}{2} M_o^2 \right] \eta$$

$$= GD \rho_o u_o C_p T_{so} \eta \qquad (90)$$

where the efficiency η is again given by

$$\eta = 1 - \frac{\frac{1}{(\gamma-1)M^2} + \frac{1}{2}}{\frac{1}{(\gamma-1)M_o^2} + \frac{1}{2}} s^2 \qquad (91)$$

The average output power density, w_e, is obtained by using equation (90) and (89) and is given by the following expression

$$\frac{w_e}{C_p T_{so} \sigma_o B^2} = \frac{\eta \, b(1 - e_L)}{\left(\frac{1}{M_o^2} - \frac{1}{M^2}\right) - (\gamma + 1) \ln s} \qquad (92)$$

where η is given by equation (91) and s by equation (85).

D. Constant Area Duct Segmented Electrodes Faraday Generator with Constant Electrical Conductivity, σ_o, and Constant Output Voltage Along the Duct

In this case the load voltage is kept constant between each pair of electrodes along the duct. Thus, $\mathcal{E}_y$ = constant = $e_L u_o B_o$ and, hence,

$$J_y = -\sigma_o u_o B(s - e_L) \tag{93}$$

Using this expression for the current density in the y-direction the equation of motion and the energy equation take on the following forms

1) Equation of Motion

$$\rho_o u_o \frac{d}{dx}\left(u + \frac{u}{\gamma M^2}\right) = J_y B_z = -\sigma_o u_o B^2 (s - e_L) \tag{94}$$

2) Energy Equation

$$\rho_o u_o \frac{d}{dx}\left\{\frac{u^2}{(\gamma - 1)M^2} + \frac{u^2}{2}\right\} = \mathcal{E}_y J_y = -u_o^2 \sigma_o B^2 e_L (s - e_L) \tag{95}$$

Equations (94) and (95) are the same as equations (20) and (21), respectively, in Ref. 1 and the solution of this case has been presented in that reference.

DISTRIBUTION LIST

	No. Copies
Director, Advanced Research Projects Agency The Pentagon Washington 25, D. C. Attn: Dr. John Huth	2
Office of Naval Research Power Branch (Code 429) Washington 25, D. C. Attn: John A. Satkowski	6
U. S. Naval Research Laboratory Washington 25, D. C. Attn: Dr. Alan Kolb, Code 7470 B. J. Wilson, Code 5230 Technical Information Division	1 1 6
Wright-Patterson Air Force Base Aeronautical Systems Division Ohio Attn: Don Warnock (ASRMFP-2)	1
Air Force Office of Scientific Research Washington 25, D. C. Attn: Dr. Milton M. Slawsky	1
U. S. Naval Ordnance Test Station Propulsion Applied Research Group China Lake, California Attn: Dr. H. Powell Jenkins, Jr.	1
Rome Air Development Center Rome, New York Attn: Mr. Frank J. Mellura	1
U. S. Naval Ordnance Laboratory NA Division White Oak, Maryland Attn: Wallace Knutsen Library	1 2
Armed Services Technical Information Agency Arlington Hall Station Arlington 12, Virginia	10
U. S. Army Research & Development Laboratory Fort Belvoir, Virginia Attn: Frank Shields (ERD-EP)	1

	No. Copies
NASA, Lewis Research Center 21000 Brookpark Road Cleveland 35, Ohio	
Attn: Wolfgang Moeckel	1
J. Howard Childs	1
U. S. Atomic Energy Commission Division of Reactor Development Direct Energy Conversion Section, RD; AED Germantown, Maryland	1
Dr. J. E. McCune Aeronautical Research Associates of Princeton Princeton, New Jersey	1
Dr. T. Brogan AVCO - Everett Research Laboratory 2385 Revere Beach Parkway Everett, Massachusetts	1
Dr. J. Cole Department of Aeronautics California Institute of Technology Pasadena, California	1
Mr. Arthur Sherman General Electric - Valley Forge Valley Forge Space Technical Center Philadelphia 1, Pa.	1
Dr. George Sutton General Electric - Valley Forge Valley Forge Space Technical Center Philadelphia 1, Pa.	1
Prof. H. H. Woodson Electrical Engineering Department Massachusetts Institute of Technology Cambridge 39, Massachusetts	1
Dr. Vernon H. Blackman MHD Research Incorporated 1535 Monrovia Street Newport Beach, California	1
Dr. B. C. Lindley Nuclear Research Centre C. A. Parsons & Co., Ltd. Fossway, Newcastle Upon Tyne 6 England	1

	No. Copies
Dr. M. C. Gourdine Curtiss Wright Wright Aeronautical Division Wood-Ridge, New Jersey	1
Dr. W. O. Carlson Radio Corporation of America Defense Electronic Products Moorestown, New Jersey	1
Dr. Robert Eustis Thermosciences Division Stanford University Stanford, California	1
Mr. W. C. Davis TRW-TAPCO Group 7209 Platt Avenue Cleveland 4, Ohio	1
Mr. Stan Markowski Pratt and Whitney Aircraft 400 Main Street East Hartford 8, Connecticut	1
Mr. Swift Hook Central Electricity Research Laboratories Cleeve Road, Leatherhead, Surrey England	1
Dr. Richard Schamberg Rand Corporation 1700 S. Main Street Santa Monica, California	1
Dr. Sam Naiditch Unified Science Associates 826 Arroyo Parkway Pasadena, California	1
Mr. Wade Dickinson Bechtel Corporation 141 Battery Street San Francisco, California	1